



## ORIGINAL ARTICLE

# Design and synthesis of some novel pyridothienopyrimidine derivatives and their biological evaluation as antimicrobial and anticancer agents targeting EGFR enzyme



Eman M. Mohi El-Deen<sup>a,\*</sup>, Manal M. Anwar<sup>a,\*</sup>, Amina A. Abd El-Gwaad<sup>a</sup>,  
Eman A. Karam<sup>b</sup>, Mohamed K. El-Ashrey<sup>c</sup>, Rafika R. Kassab<sup>d,e</sup>

<sup>a</sup> Department of Therapeutic Chemistry, National Research Centre, Dokki, Cairo 12622, Egypt

<sup>b</sup> Department of Microbial Chemistry, National Research Centre, Dokki, Cairo 12622 Egypt

<sup>c</sup> Department of Pharmaceutical Chemistry, Faculty of Pharmacy, Cairo University, Cairo 11562, Egypt

<sup>d</sup> Department of Chemistry, Faculty of Science, Al-Azhar University, Cairo 11754, Egypt

<sup>e</sup> Department of Chemistry, Faculty of Science (Girls), Al-Azhar University, Cairo 11754, Egypt

Received 2 October 2021; accepted 27 January 2022

Available online 1 February 2022

## KEYWORDS

Pyridothienopyrimidines;  
Antimicrobial activity;  
Anticancer activity;  
EGFR inhibitors

**Abstract** A new series of pyridothienopyrimidine derivatives was designed and evaluated as antimicrobial and anticancer agents. The target compounds were synthesized starting with 3-amino thieno[2,3-b]pyridine-2-carboxamide derivative **1** which underwent cyclocondensation reaction with aromatic aldehydes to give the key intermediates **2a,b**. By further treatment of **2a,b** with various reagents, the target 2,4-disubstituted-pyrido[3',2':4,5]thieno[2,3-d]pyrimidines **3a,b–11a,b** were obtained. To evaluate the antimicrobial activity of the new compounds, they were tested against five bacterial and five fungal strains. Compounds **6c**, **8b**, **9a** and **9b** revealed the most significant antimicrobial activity against the tested microorganisms with MIC values range (4–16 µg/mL). Also, compounds **2a,b–11a,b** were screened for their *in vitro* cytotoxic activity against HepG-2 and MCF-7 cancer cell lines compared with doxorubicin and cisplatin as references drugs. Moreover, compounds (**2b**, **4a**, **6a**, **7b**, **7c** and **9a**) which exhibited the most potent anticancer activity, were further subjected to EGFR<sup>WT</sup> enzyme inhibition assay utilizing erlotinib as a standard drug. The compounds **6a**, **7b**, **7c** and **9a** which showed the most promising suppression effects were also evaluated as inhibitors against the mutant forms EGFR<sup>L858R</sup> and EGFR<sup>T790M</sup>. The 4-aminopyrazolone analogue **9a** showed superior anticancer activity against both HepG-2 and MCF-7 cell lines

\* Corresponding authors.

E-mail addresses: e.mohi.2010@live.com (E.M. Mohi El-Deen), manal.hasan52@live.com (M.M. Anwar).

Peer review under responsibility of King Saud University.



Production and hosting by Elsevier

(IC<sub>50</sub> = 1.27, 10.80 μM, respectively) and more potent enzymatic inhibition activity against EGFR<sup>WT</sup> and its mutant forms EGFR<sup>L858R</sup> and EGFR<sup>T790M</sup> than that obtained by erlotinib (IC<sub>50</sub> = 0.021, 0.053, 0.081 μM, respectively, IC<sub>50erlotinib</sub>; 0.027, 0.069, 0.550 μM, respectively). Finally, the molecular docking study showed good binding patterns of the most active compounds with the prospective target EGFR<sup>WT</sup>.

© 2022 The Author(s). Published by Elsevier B.V. on behalf of King Saud University. This is an open access article under the CC BY-NC-ND license (<http://creativecommons.org/licenses/by-nc-nd/4.0/>).

## 1. Introduction

Cancer disease represents a serious threat to human health due to its massive and complicated etiology (Wu et al., 2018). Liver cancer is a global health issue representing the sixth most common cancer type, and the third leading reason for cancer-related death. Furthermore, 75%–85% of liver cancer cases include hepatocellular carcinoma (HCC) (Sung et al., 2021). Although the spread of HCC, few drugs are available for its clinical treatment, especially in the advanced stages, thereby many efforts should be made in the development of new drugs for this serious cancer type (Luo et al., 2021). On the other hand, breast cancer (BC) is the world's most prevalent cancer resulting in about 14% of the cancer-related deaths among women (Sung et al., 2021, Presti and Qua Quarini, 2019). Despite the recent discovery of several promising novel therapies which exhibited considerable therapeutic success, drug resistance still remains one of the most important challenges in BC treatment (Lainetti et al., 2020).

Moreover, many recent studies exhibited that epidermal growth factor receptor (EGFR) was generally altered in many types of cancers. Thus, the inhibition of EGFR's kinase activity became a primary target for developing many cancer therapeutics (Thomas and Weihua, 2019). In clinical use, there are many small molecules acting as EGFR inhibitors such as: Osimertinib (AZD9291), olmutinib, PF06747775, WZ4002, Rociletinib, Nazartinib and others belong to the 3rd generation of EGFR kinase inhibitors (Liang et al., 2021; Phan et al., 2019). However, various side effects have been detected with their uses in the clinical application (Shah and Shah, 2019; Wang and Cang, 2016). Also, several mechanisms of resistance have been described to EGFR-TKIs, such as secondary and tertiary mutations in the EGFR gene T790M and C797S, respectively (Morgillo et al., 2016; Jänne et al., 2015). Accordingly, many efforts are still required to reach new EGFR inhibitors which can overcome resistance mechanisms and have high selectivity to minimize the adverse effects.

In addition, the immunosuppression, which usually results due to the anticancer drug regimen and the destruction of the mucosal barrier due to utilizing invasive devices in cancer patients making them at risk of different infectious diseases that need long-term prophylactic antibiotics (Sharma et al., 2021). Thus, there is an increasing urgency in designing novel anticancer agents having dual anticancer and antimicrobial activities to protect cancer patients against microbial infections (Felicio et al., 2017).

Thieno[2,3-*b*]pyridine nucleus plays a vital role in the field of drug discovery, producing a wide spectrum of biological activities such as; anticancer (Abdelaziz et al., 2018; Arabshahi et al., 2015; Eurtivong et al., 2017; Al-Trawneh et al., 2021), antimicrobial (Ghattas et al., 2015; Mohi El-

Deen et al., 2019; Mansour, 2020), antiviral (Amorim et al., 2017; Schnute et al., 2007), anti-inflammatory (Liu et al., 2013; Madhusudana et al., 2012), and antiangiogenic (Rizka et al., 2019) activities. In addition, the strategies of different new studies have been directed to the synthesis of compounds bearing thieno[2,3-*b*]pyridine fused with pyrimidine ring giving rise to the pyrido[3',2':4,5]thieno[3,2-*d*] pyrimidine scaffold as significant anticancer (Aziz et al., 2015a; Sirakanyan et al., 2019) and antimicrobial candidates (Mohi El-Deen et al., 2020; Ge Zayda et al., 2020; Sanad and Mekky, 2021; Fayed et al., 2014; El-Essawy et al., 2016) (Fig. 1).

Moreover, many biological studies revealed that the pyridothienopyrimidine-based derivatives produce their anticancer activities via protein kinase suppression effects such as; Pim-1 kinase, casein kinase 1 (CK1), dual-specificity protein kinase (CLK1), vascular endothelial growth factor receptor (VEGFR-2), and EGFR kinase (El-Nassan et al., 2018; Loidreau et al., 2012; Aziz et al., 2015b).

It has been reported that there are four essential pharmacophoric features shared by the reported and clinically used EGFR-TKIs: (i) a flat heterocyclic-aromatic ring system (ii) a terminal hydrophobic head (iii) NH-linker (iv) a hydrophobic tail (Elmetwally et al., 2019). Chia-Hsien Wu et al., have synthesized compound **VII** utilizing a knowledge-based design procedure for ATP-competitive inhibitors binding with the active site of the EGFR-TK. This compound showed high efficacy for suppressing the targeted enzyme, EGFR-TK (Wu et al., 2010). Furthermore, Milik et al. have reported the thieno[2,3-*d*]pyrimidine compound **VIII** as a potent anticancer agent targeting EGFR and HER2-TK (Milik et al., 2018) (Fig. 2).

In view of the above issues, this work deals with the design and synthesis of a new series of pyridothienopyrimidine compounds (**2a,b–11a,b**) as antimicrobial and as anticancer agents bearing the reported essential pharmacophoric features of EGFR-TKIs. As the thieno[3,2-*d*]pyrimidine sector of the pyridothienopyrimidine represents the central hetero-aromatic ring since the nitrogen atoms of the pyrimidine ring serve as hydrogen-bond acceptors resulting in promising EGFR-TK inhibitory potency. While, the substituent at position-4 was the linker (spacer) area, where the length of the linker in addition to the number of its hydrogen-bond acceptor and/or hydrogen-bond donor groups was modified. The different linkers were NH as compounds **5a,b**, **6a–c**, NH-N = C as **7a–c** as well as a direct attachment with pyrazoline-N as compounds **8a,b–11a,b** was also carried out in order to study its positive or negative impact on the target enzyme inhibition activity. The hydrophobic tail was based on the pyridine nucleus to occupy the front hydrophobic region of the ATP binding site. Also, the hydrophobic head is an alkyl or aryl group (Elmetwally et al., 2019, Nasser et al., 2020) (Fig. 2).

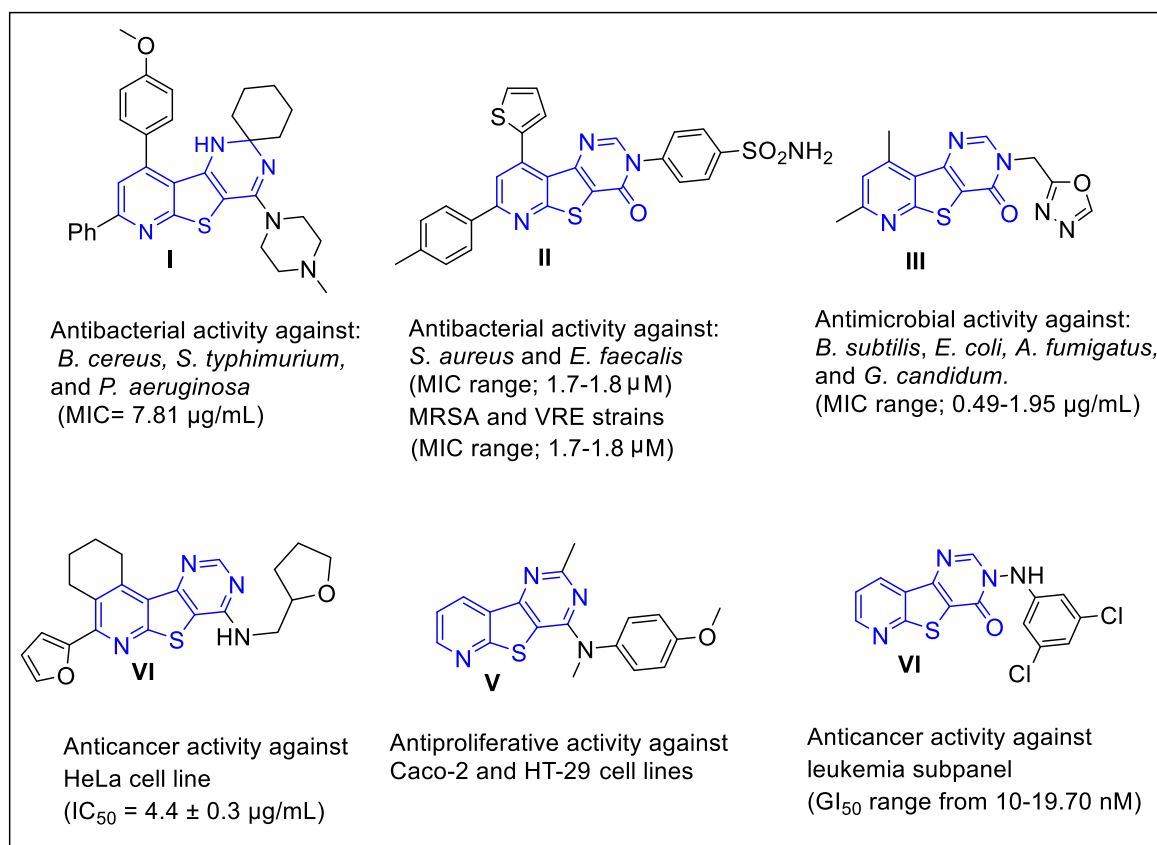


**Fig. 1** Some previously synthesized pyridothienopyrimidine derivatives as antimicrobial agents (I-III) and as anticancer agents (IV-VI).

Next, all the target compounds were evaluated as antimicrobial agents against a panel of gram-positive, gram-negative bacterial, yeast and fungal strains. Also, the target compounds were assessed as anticancer agents against human liver carcinoma cell line (HepG2) and human breast cancer cells (MCF-7). The safety of the most potent anticancer candidates (**2b**, **4a**, **6a**, **7b**, **7c** and **9a**) was evaluated against the normal WISH cell line. In addition, these compounds were further evaluated for their ability to suppress EGFR kinase. Also, molecular docking study was conducted to find out the plausible binding modes of the most promising derivatives in the active pocket of EGFR.

## 2. Results and discussion

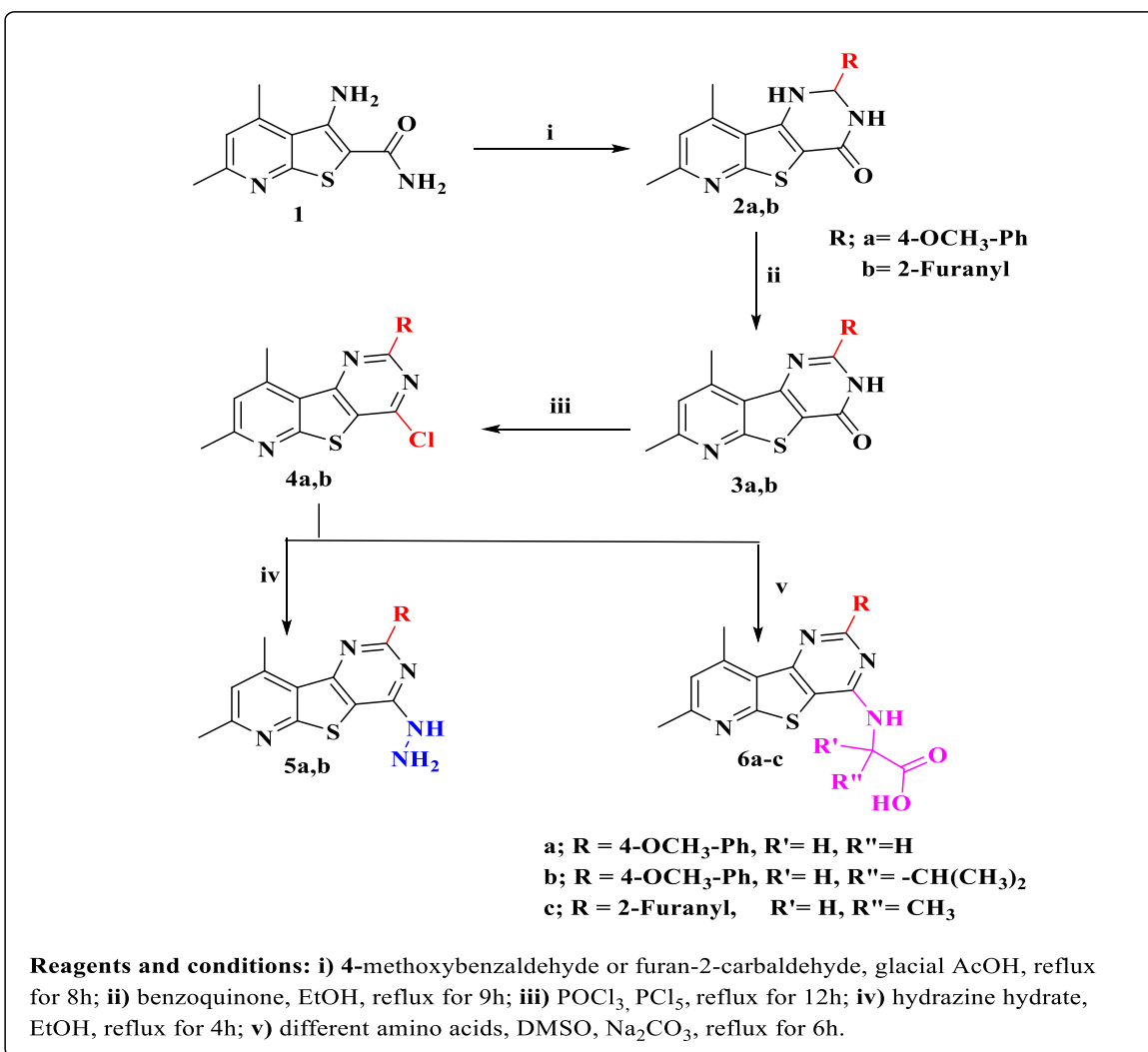
### 2.1. Chemistry

The new set of pyridothienopyrimidine derivatives (**2a,b-11a,b**) was prepared utilizing the synthetic pathways outlined in Schemes 1, 2. The molecular structures of all the new compounds were confirmed via spectral data (IR, <sup>1</sup>H NMR, <sup>13</sup>C NMR and Mass) and elemental microanalyses. The bicyclic compound 3-amino-4,6-dimethylthieno[2,3-b]pyridine-2-carboxamide (**1**) (Youssefyeh, et al., 1984) was refluxed with aldehydes (4-methoxybenzaldehyde or furan-2-carbaldehyde) in glacial acetic acid to give, via cyclocondensation reaction, the tricyclic compounds 2,3-dihydropyridothienopyrimidin-4

(1*H*)-ones **2a,b**. Upon treatment of **2a,b** with benzoquinone as an oxidizing agent, they underwent dehydrogenation to give the pyridothienopyrimidin-4(3*H*)-ones **3a,b**. Subsequently, the latter derivatives **3a,b** were treated with POC<sub>1</sub><sub>3</sub>/PCl<sub>5</sub> mixture to yield the corresponding 4-chloro derivatives **4a,b** (Scheme 1).

The tricyclic structures of **2a,b** were confirmed by <sup>1</sup>H NMR spectra of **2a** and **2b**, they showed the signals of the aromatic protons of the appropriate aldehyde at δ 6.31–7.61 ppm alongside the two singlets signals corresponding to the two pyrimidinone NH groups at δ (7.02, 8.32 ppm) and δ (7.16, 8.35 ppm), respectively. Also, <sup>1</sup>H NMR spectra of **2a** and **2b** revealed a singlet signal at δ 5.81 ppm and at δ 5.90 ppm corresponding to the CH of the pyrimidinone ring. The vanishing of one signal of the two singlets signals corresponding to the two pyrimidinone NH groups with the CH-pyrimidinone signal in the <sup>1</sup>H NMR spectra of **3a,b** confirmed the dehydrogenation reaction of **2a,b**. The signal of the other NH group appeared as a downfield singlet at δ 12.83 and 13.0 ppm in the spectra of **3a** and **3b**, respectively, which indicated the presence of NH adjacent to the C = O group and confirmed the 1,2-dehydrogenation of **2a,b** instead of the 2,3-dehydrogenation. Also, the <sup>13</sup>C NMR spectra of **2a,b** and **3a,b** gave additional support to their structures. In the <sup>13</sup>C NMR spectra of **2a,b** the signals of CH-pyrimidinone appeared at δ 61.41–66.13 ppm and shifted downfield with the aromatic carbons in the <sup>13</sup>C NMR spectra of **3a,b**. Moreover, the IR and <sup>1</sup>H NMR spectra of the 4-





**Scheme 1** Synthesis of new pyrido[3',2':4,5]thieno[3,2-*d*]pyrimidine-based compounds **2a,b-6a-c**.

pyrazolone derivatives **9a,b**, **10a,b** and the 4-pyrazole derivatives **11a,b**; respectively (Scheme 2).

The molecular structures of the 4-pyrazolone compounds **9a,b** and **10a,b** were confirmed by the existence of a singlet signal at the range  $\delta$  2.97–3.06 ppm corresponding to the pyrazolone-CH<sub>2</sub> in their <sup>1</sup>H NMR spectra. On the other hand, an additional band at 1695–1674 cm<sup>-1</sup> for the C = O group of the pyrazolone nucleus was found in their IR spectra. Also, <sup>13</sup>C NMR spectra of **9a,b** and **10a,b** represented a signal at the range  $\delta$  170.17–172.92 ppm assignable for pyrazolone-C = O group. Furthermore, <sup>1</sup>H NMR spectra of the 4-pyrazole derivatives **11a,b** showed four singlet signals at the range  $\delta$  2.22–2.99 ppm referring to the pyrazole-2CH<sub>3</sub> in addition to the parent pyridine-2CH<sub>3</sub>. Also, the four signals of the 4CH<sub>3</sub> of **11a,b** were exhibited in their <sup>13</sup>C NMR spectra at the range  $\delta$  13.72–24.71 ppm alongside the parent signals. Further support for the suggested structures of the new compounds was gained by their mass spectra, which were in accordance with the proposed structures representing their correct molecular ion peaks.

## 2.2. Biological evaluation

### 2.2.1. Antimicrobial activity

Since the strategy of our work was based on achieving new pyrido[3',2':4,5]thieno[3,2-*d*]pyrimidine compounds possessing dual cytotoxic and antimicrobial activities, all the new compounds were evaluated as antimicrobial agents versus a panel of microbial strains. They were examined against three gram-positive bacteria viz. *Staphylococcus aureus* 25923, *Bacillus subtilis* 6633, *Bacillus cereus* 33018, two gram-negative bacteria viz. *Escherichia coli* 8739, *Salmonella typhimurium* 14028, three yeasts viz. *Candida albicans* 10231, *Candida tropicalis* 750, *Saccharomyces cerevisiae* and two fungi viz. *Aspergillus flavus*, *Aspergillus niger* EM77 (KF774181). The zones of inhibition in (mm) and the MIC values in (μg/mL) were determined for the target compounds and the reference drugs Amoxicillin trihydrate and clotrimazole (Table 1 and 2).

On the basis of the MIC values, it is apparent that there was wide variability in the antimicrobial potency of the evaluated derivatives. It has been found that the derivatives; alanine



**Table 1** *In vitro* antibacterial activities of the synthesized compounds expressed as mean diameter of inhibition zones in mm and MICs ( $\mu\text{g/mL}$ ) against the tested pathogenic bacteria.

Compd. No.	Gram + ve Bacteria			Gram-ve Bacteria	
	<i>S. aureus</i> 25,923	<i>B. subtilis</i> 6633	<i>B. cereus</i> 33,018	<i>E. coli</i> RCMB 010,052	<i>S. typhimurium</i> ATCC 14,028
2a	20 (64)	18 (64)	N.A.	N.A.	N.A.
2b	27 (32)	23 (64)	23 (32)	22 (64)	21(64)
3a	14 (128)	14 (128)	NA	NA	NA
3b	12 (128)	13 (128)	NA	NA	NA
4a	22 (64)	17 (64)	21 (64)	28 (8)	27 (16)
4b	24 (64)	21 (64)	22 (32)	26 (32)	24 (32)
5a	19 (64)	18 (64)	14 (128)	12 (128)	11 (128)
5b	20 (64)	25 (32)	24 (32)	19 (64)	18 (128)
6a	35 (4)	32 (8)	29 (16)	27 (16)	31 (16)
6b	19 (64)	24 (32)	20 (64)	22 (64)	24 (64)
6c	25 (32)	28 (16)	25 (32)	27 (8)	26 (16)
7a	13 (128)	25 (32)	19 (64)	23 (32)	21(64)
7b	25 (32)	26 (32)	22 (64)	20 (64)	20 (64)
7c	27 (16)	25 (16)	27 (32)	14 (64)	28 (16)
8a	24 (32)	22 (64)	22 (64)	23 (64)	20 (64)
8b	30 (4)	29 (8)	28 (16)	30 (8)	28 (16)
9a	33 (4)	29 (8)	31 (16)	27 (8)	30 (16)
9b	28 (8)	26 (16)	25 (16)	26 (8)	28 (16)
10a	25 (64)	24 (32)	24 (32)	18 (64)	20 (64)
10b	22 (64)	N.A.	13 (128)	16 (64)	N.A.
11a	24 (32)	25 (32)	22 (64)	24 (64)	27 (32)
11b	26 (32)	24 (32)	21 (32)	25 (32)	25 (32)
Amoxicillin Trihydrate	30(4)	29(8)	28 (16)	27 (8)	28 (16)

N.A. = No Activity (mean diameter of inhibition zones < 11 mm).  
Minimum Inhibitory Concentrations (MIC) ( $\mu\text{g/mL}$ ).

orubicin and cisplatin served as reference drugs. The concentrations of the compounds that induced 50% inhibition of cell viability ( $\text{IC}_{50}$ ,  $\mu\text{M}$ ) were determined and listed in Table 3.

**2.2.2.1. Structure-activity relationship (SAR).** The biological data revealed that the tested derivatives displayed more promising cytotoxic activity against HepG2 cancer cell line of  $\text{IC}_{50}$  range; 1.81–48.70  $\mu\text{M}$  more than MCF-7 cells of  $\text{IC}_{50}$  range 10.80–80.61  $\mu\text{M}$ , compared to doxorubicin of  $\text{IC}_{50}$ s; 2.85, 3.58  $\mu\text{M}$ , respectively. With respect to HepG2, it has been noted that the conjugation of the aminopyrazolinone nucleus to the parent 2-(4-methoxyphenyl)-pyridothienopyrimidine scaffold as compound **9a** exhibited 2.2 folds more significant activity than doxorubicin of  $\text{IC}_{50}$  value; 1.27  $\mu\text{M}$ ,  $\text{IC}_{50}$ doxorubicin 2.85  $\mu\text{M}$ . Furthermore, tagging the latter parent core with glycine amino acid as compound **6a** represented 1.5 folds more potent cytotoxic activity than the reference drug of  $\text{IC}_{50}$  value; 1.80  $\mu\text{M}$ . Also, the Schiff's bases **7b,c** revealed slightly more potent cytotoxicity than that of doxorubicin with  $\text{IC}_{50}$ s; 2.63, 2.15  $\mu\text{M}$ , respectively. While, the parent **2b**, the 4-chloro derivative **4a**, the tetracyclic pyridothienotriazolopyrimidine derivative **8a** and the valine amino acid derivative **6b** showed a slight decrease in the potency than the reference drug with  $\text{IC}_{50}$  values; 3.11–4.02  $\mu\text{M}$  respectively. Additionally, the resultant data also showed that the 4-pyrazolone derivative **9b**, the pyridothienopyrimidin-4-one derivative **3a**, the 4-hydrazino

derivative **5b** and the tetracyclic **8b** produced cytotoxic activity ranging from half to third that of doxorubicin with  $\text{IC}_{50}$  values range; 5.71–8.37  $\mu\text{M}$ . A further apparent decrease in the cytotoxicity was observed by the rest of the compounds (**2a**, **3b**, **4b**, **5a**, **6c**, **7a**, **10a,b** and **11a,b**), they gave a wide variety of  $\text{IC}_{50}$  values ranging from 9.02 to 48.70  $\mu\text{M}$ .

On the other hand, MCF-7 cancer cells appeared to be less sensitive to the tested compounds in comparing to doxorubicin. Whereas, all the target compounds exhibited lower cytotoxicity with  $\text{IC}_{50}$  values range; 10.80–80.61  $\mu\text{M}$  than that of doxorubicin with  $\text{IC}_{50}$  value; 3.58  $\mu\text{M}$ . While taking cisplatin as a reference drug, most of the evaluated derivatives represented promising cytotoxic effects. Fortunately, the 4-pyrazolone derivative **9a**, the most potent cytotoxic agent against HepG2 cancer cell line, was the most potent agent against MCF-7 cancer cells with  $\text{IC}_{50}$ ; 10.80  $\mu\text{M}$  compared with  $\text{IC}_{50}$ cisplatin; 20.70  $\mu\text{M}$ . Moreover, the parent pyridothienopyrimidin-4-one **2b**, the 4-chloro analogue **4a**, the glycine derivative **6a** and the Schiff's bases **7c** exhibited more potent activity than cisplatin with  $\text{IC}_{50}$  values range; 11.07–19.70  $\mu\text{M}$ . Approximate equipotent activity to that of the reference drug cisplatin was gained by the compounds **2a**, **4b**, **6b**, **7a**, **7b**, **8b** and the 4-pyrazole derivative **11b** of  $\text{IC}_{50}$  values; 20.51–23.80  $\mu\text{M}$ . While, the rest derivatives (**3a,b**, **5a,b**, **6c**, **8a**, **10a,b**, **11a**) exhibited less potent activity than cisplatin with  $\text{IC}_{50}$  values range; 28.03–80.61  $\mu\text{M}$ .

**Table 2** *In vitro* antifungal activities of the synthesized compounds expressed as mean diameter of inhibition zones in mm and MICs ( $\mu\text{g}/\text{mL}$ ) against the tested pathogenic fungi.

Compd. No.	Yeasts			Fungi	
	<i>C. albicans</i> ATCC 10,231	<i>C. tropicalis</i> ATCC 750	<i>S. cerevisiae</i>	<i>A. flavus</i>	<i>A. niger</i> EM77 (KF774181)
2a	NA	NA	22 (32)	28 (32)	26 (32)
2b	22 (64)	21 (64)	23 (32)	25 (32)	26 (32)
3a	N.A.	N.A.	16 (128)	11 (128)	14 (64)
3b	N.A.	N.A.	15 (128)	N.A.	N.A.
4a	29 (8)	28 (8)	21 (64)	27 (32)	17 (64)
4b	27 (32)	24 (32)	24 (32)	17 (64)	19 (64)
5a	18 (128)	14 (128)	17 (128)	11 (128)	14 (128)
5b	19 (64)	18 (128)	17 (64)	23 (32)	22 (64)
6a	29 (8)	31 (8)	37 (8)	33 (8)	35 (8)
6b	26 (64)	24 (64)	16 (128)	14 (128)	18 (64)
6c	32 (8)	29 (8)	36 (8)	29 (16)	28 (16)
7a	23 (64)	22 (64)	24 (32)	18 (64)	19 (64)
7b	20 (64)	20 (64)	23 (32)	15 (64)	14 (64)
7c	30 (8)	28 (8)	20 (64)	30 (8)	29(8)
8a	24 (32)	26 (32)	24 (32)	18 (64)	18(64)
8b	30 (8)	30 (8)	37 (8)	35 (8)	36 (8)
9a	33 (8)	28 (8)	35 (8)	31 (8)	30 (8)
9b	37 (8)	33 (8)	33 (8)	28(16)	27 (16)
10a	23 (64)	14 (128)	24 (32)	18 (64)	20 (64)
10b	22 (64)	N.A.	18(64)	15 (64)	17 (64)
11a	21 (64)	24 (32)	19 (64)	26 (32)	22 (64)
11b	24 (32)	23 (32)	21 (64)	22 (32)	21 (64)
Clotrimazole	28 (16)	30 (8)	35 (8)	30(8)	31 (8)

N.A. = No Activity (mean diameter of inhibition zones < 11 mm).  
Minimum Inhibitory Concentrations (MIC) ( $\mu\text{g}/\text{mL}$ ).

Since the frequency and the severity of the adverse effects to the normal healthy cells at therapeutic levels is considered as one of the most critical factors that characterize different anti-cancer drugs from each other, the target compounds **2b**, **4a**, **6a**, **7b**, **7c** and **9a**, which revealed the most potent cytotoxic activity against both of HepG2 and MCF-7 cancer cell lines were selected to evaluate their cytotoxic activity against the normal human amnion-derived (WISH) cell line via MTT assay to determine their safety profiles. The tested compounds showed low toxicity against the normal cells with  $\text{IC}_{50}$  values ranging from 107.01 to 494.10  $\mu\text{M}$ , which are much higher than their  $\text{IC}_{50}$  values range 1.27–20.51  $\mu\text{M}$  against the cancer cell lines (Table 3) confirming their promising safety profile.

### 2.2.3. *In vitro* enzyme inhibition assay of EGFR<sup>WT</sup>, EGFR<sup>L858R</sup> and EGFR<sup>T790M</sup>

Several reports indicated that high expression of EGFR is detected in breast cancer and hepatocellular carcinoma (Shetty et al., 2021; Song et al., 2017; Masuda et al., 2012). Thus, EGFR<sup>WT</sup> kinase assay was performed for the target pyridothienopyridine compounds (**2b**, **4a**, **6a**, **7b**, **7c** and **9a**), which investigated the most potent cytotoxic activities against both MCF-7 and HepG-2 cancer cells in order to study their postulated mechanism of action. Erlotinib as one of the most potent EGFR<sup>WT</sup> inhibitors was utilized as a reference drug (Lyseng-Williamson, 2010) and the results were expressed as  $\text{IC}_{50}$  values ( $\mu\text{M}$ ) (Table 4). Interestingly, all the tested derivatives showed promising inhibitory activity of EGFR<sup>WT</sup> kinase

with  $\text{IC}_{50}$  values range; 0.021–0.117  $\mu\text{M}$ . The resultant data demonstrated that the 4-aminopyrazolone derivative **9a** as EGFR<sup>WT</sup> inhibitor was more potent than the standard drug of  $\text{IC}_{50}$ ; 0.021  $\mu\text{M}$ ,  $\text{IC}_{50}$  erlotinib; 0.027  $\mu\text{M}$ . Also, the Schiff's base **7c** showed significant kinase inhibitory activity with  $\text{IC}_{50}$  = 0.032  $\mu\text{M}$ , which decreased slightly than Erlotinib. Whereas, the glycine derivative **6a** and the Schiff's base **7b** revealed further lowering in the inhibitory activity with  $\text{IC}_{50}$  values; 0.046, 0.051  $\mu\text{M}$ , respectively. However, the precursor 4-chloro analogue **4a** appeared to be 3 folds less potent than Erlotinib with  $\text{IC}_{50}$ ; 0.083  $\mu\text{M}$ . Also, a detectable drop was also recognized by the pyrimidin-4-one derivative **2b** which revealed  $\text{IC}_{50}$ ; 0.117  $\mu\text{M}$ . It was obvious that the nitrogen of the pyrazolone ring in **9a** and the nitrogen in the side chains, as the glycine amino acid of **6a** and the hydrazide Schiff's base of **7b** and **7c**, which attached at position-4 of the parent pyridothienopyrimidine system, provide an important role in EGFR suppression.

Furthermore, the compounds representing the most potent inhibitory activity against EGFR<sup>WT</sup>; **6a**, **7b**, **7c**, **9a** were also evaluated as inhibitors against the mutant forms EGFR<sup>L858R</sup> and EGFR<sup>T790M</sup> in comparison to erlotinib as a reference drug. The obtained results were summarized in Table 5. It has been observed that the 4-aminopyrazolone derivative **9a** displayed more potent inhibitory activity than erlotinib against both mutant forms EGFR<sup>L858R</sup> and EGFR<sup>T790M</sup> of  $\text{IC}_{50}$ s = 0.053, 0.081  $\mu\text{M}$ , respectively,  $\text{IC}_{50}$  erlotinib = 0.069, 0.550  $\mu\text{M}$ , respectively. On the other hand, the Schiff's base

**Table 3** *In vitro* cytotoxic activity of the new compounds towards HepG2 and MCF-7 cell lines.

Compound No.	IC <sub>50</sub> (μM)		
	HepG-2	MCF-7	WISH
2a	11.01 ± 0.75	23.02 ± 1.76	
2b	3.11 ± 0.21	12.90 ± 0.70	494.00 ± 17.90
3a	5.71 ± 0.32	60.30 ± 3.85	
3b	15.10 ± 1.03	35.60 ± 3.03	
4a	3.17 ± 0.22	11.07 ± 0.19	107.01 ± 4.20
4b	48.70 ± 3.34	21.70 ± 0.85	
5a	13.01 ± 0.89	28.03 ± 1.75	
5b	8.37 ± 0.51	71.61 ± 3.51	
6a	1.80 ± 0.12	14.21 ± 0.22	121.02 ± 5.10
6b	4.02 ± 0.37	22.50 ± 1.90	
6c	17.80 ± 1.22	29.66 ± 2.65	
7a	21.30 ± 1.46	23.80 ± 2.80	
7b	2.63 ± 0.18	20.51 ± 2.30	302.00 ± 11.40
7c	2.15 ± 0.15	19.71 ± 1.60	213.01 ± 7.50
8a	3.93 ± 0.27	41.10 ± 3.30	
8b	6.10 ± 0.42	22.40 ± 2.70	
9a	1.27 ± 0.09	10.80 ± 0.74	278.02 ± 9.70
9b	5.73 ± 0.39	38.11 ± 3.02	
10a	17.40 ± 1.20	80.61 ± 3.95	
10b	9.02 ± 0.48	64.60 ± 2.90	
11a	9.68 ± 0.66	20.80 ± 1.08	
11b	16.30 ± 1.12	36.61 ± 3.20	
Doxorubicin	2.85 ± 0.21	3.58 ± 0.33	432.10 ± 19.30
Cisplatin	—	20.70 ± 0.83	

7c employed lower activity than that of erlotinib against EGFR<sup>L858R</sup> of IC<sub>50</sub> = 0.252 μM, but its activity surpassed the reference drug by 2.5 times against the mutant EGFR<sup>T790M</sup> of IC<sub>50</sub> = 0.219 μM. A detectable reduction in the inhibitory activity against both mutant forms by the glycine derivative 6a and the Schiff's base 7b which appeared less potent than erlotinib representing IC<sub>50</sub>s = 1.132, 0.801 μM and 0.361, 0.719 μM, respectively.

In the light of the gained data, compounds 9a, 7c could be considered as basic scaffolds for the generation of further new candidates used for the treatment of different cancer types harboring EGFR<sup>T790M</sup> or EGFR<sup>L858R</sup> mutations, thus might overcome EGFR-TKIs drug resistance.

**Table 4** *In vitro* enzymatic inhibitory activities against EGFR<sup>WT</sup> kinase.

Compound No.	EGFR <sup>WT</sup> IC <sub>50</sub> (μM)
2b	0.117 ± 0.014
4a	0.083 ± 0.009
6a	0.046 ± 0.003
7b	0.051 ± 0.008
7c	0.032 ± 0.007
9a	0.021 ± 0.004
Erlotinib	0.027 ± 0.005

**Table 5** *In vitro* enzymatic inhibitory activities against EGFR<sup>L858R</sup> and EGFR<sup>T790M</sup>.

Compound No.	EGFR <sup>L858R</sup> IC <sub>50</sub> (μM)	EGFR <sup>T790M</sup> IC <sub>50</sub> (μM)
6a	1.132 ± 0.060	1.801 ± 0.079
7b	0.361 ± 0.020	0.719 ± 0.032
7c	0.252 ± 0.010	0.219 ± 0.010
9a	0.053 ± 0.005	0.081 ± 0.004
Erlotinib	0.069 ± 0.006	0.550 ± 0.090

### 2.3. Computational studies

#### 2.3.1. Molecular docking study

Molecular modeling studies were performed to study the binding mode of compounds (2b, 4a, 6a, 7b, 7c, and 9a) to the active sites of the target EGFR<sup>WT</sup> compared with erlotinib as an EGFR inhibitor using (MOE, 2019.0102) software. At the first, from the protein data bank (<https://www.rcsb.org/structure/1M17>), the X-ray crystallographic structure of EGFR<sup>WT</sup> kinase domain complexed with erlotinib (PDB ID: 1 M17) was downloaded. Then the binding interaction of erlotinib to the EGFR<sup>WT</sup> active site was examined. It showed strong bond interactions with Leu768 & Met769, moreover, it formed hydrogen bonds through a water molecule to Cys751, Thr766 & Thr830 (Fig. 3).

The Docking setup was first established by self-docking of the co-crystallized ligand erlotinib in the vicinity of the binding site of the enzyme. The root mean square deviation (RMSD) was 1.03086 Å and erlotinib docking score was -11.7806 kcal/mol (Fig. 4).

While, all the tested compounds showed good binding energy scores indicating their fitness in the binding pocket of the enzyme. Compounds, 9a, 7c and 6a showed the highest binding scores (-13.82, -13.56 & -13.31 kcal/mol, respectively). The 4-pyrazolone derivative 9a showed strong hydrogen bond interactions through both nitrogen atoms of the pyrimidine ring with Val702 amino acid which also showed binding with the pyrazole nitrogen. Furthermore, Lys721 bound to S atom of the thiophene ring and finally Met769 amino acid bound to CH of benzene ring and the methoxy group through non-classical hydrogen bonding. Moreover, the nitrogen atoms of the pyrimidine ring of the Schiff's base 7c exhibited hydrogen-bond interactions with Leu694 amino acid, the sulphur atom of thiophene ring bound to Leu820 Asp831 amino acids and to Thr830 via a water molecule and also, the imine nitrogen atom bound to Cys751 & Thr766 through water molecules. Through water molecules, the glycine derivative 6a interacted with Cys751, Thr766, Thr830 amino acids, while the pyridine nitrogen bound to Leu768 (Table 6 & Figs. 5-7).

#### 2.3.2. ADME study

Six physicochemical parameters were studied for the tested compounds 2a, 4a, 6a, 7b, 7c, and 9a which are Lipophilicity (LIPO), Size, Polarity (POLAR), Insolubility (INSOL), Unsaturation (UNSAT), and Flexibility (FLEX). The results are presented in the bioavailability radar chart (Fig. 8), in which the pink-colored zone indicates the suitability of

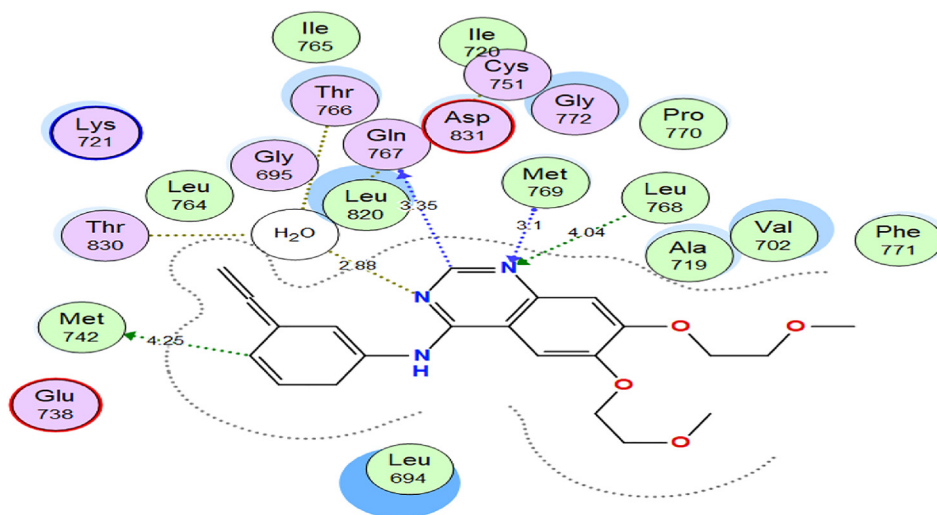


Fig. 3 2D interactions of ERL within EGFR<sup>WT</sup> active site.

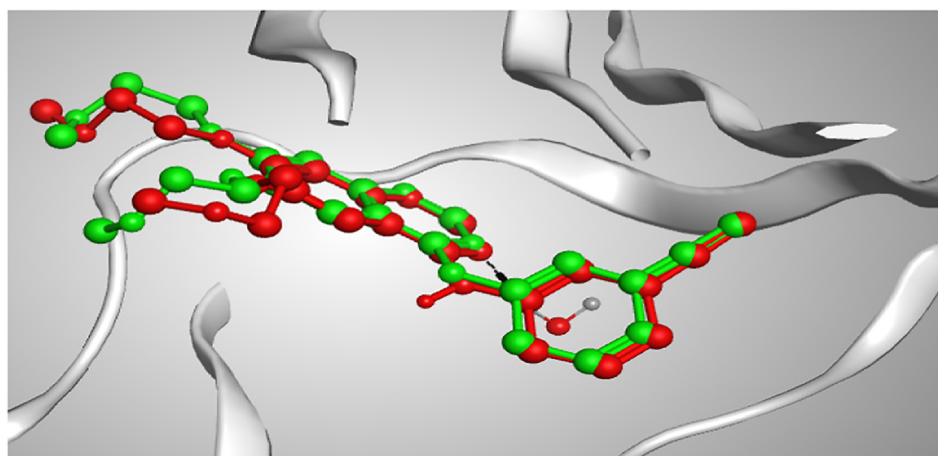


Fig. 4 3D representation of the superimposition of the co-crystallized (red) and the docking pose (green) of erlotinib in the active site of EGFR<sup>WT</sup> enzyme.

physicochemical properties to have a good *in vivo* bioavailability. All the tested derivatives showed only one violation which indicates a good bioavailability profile except compound **7b** which revealed two violations that decreased its probability in a good bioavailability outline.

The calculated water solubility displayed that all derivatives of moderate solubility except compounds **7b** and **7c** which were poorly water soluble. The predicted log P values were intermediate (2.51 for **2b**, 3.15 for **6a**, 3.24 for **9a**), slightly high for **4a** (4.71), **7c** (4.63) and high for **7b** compound (5.39).

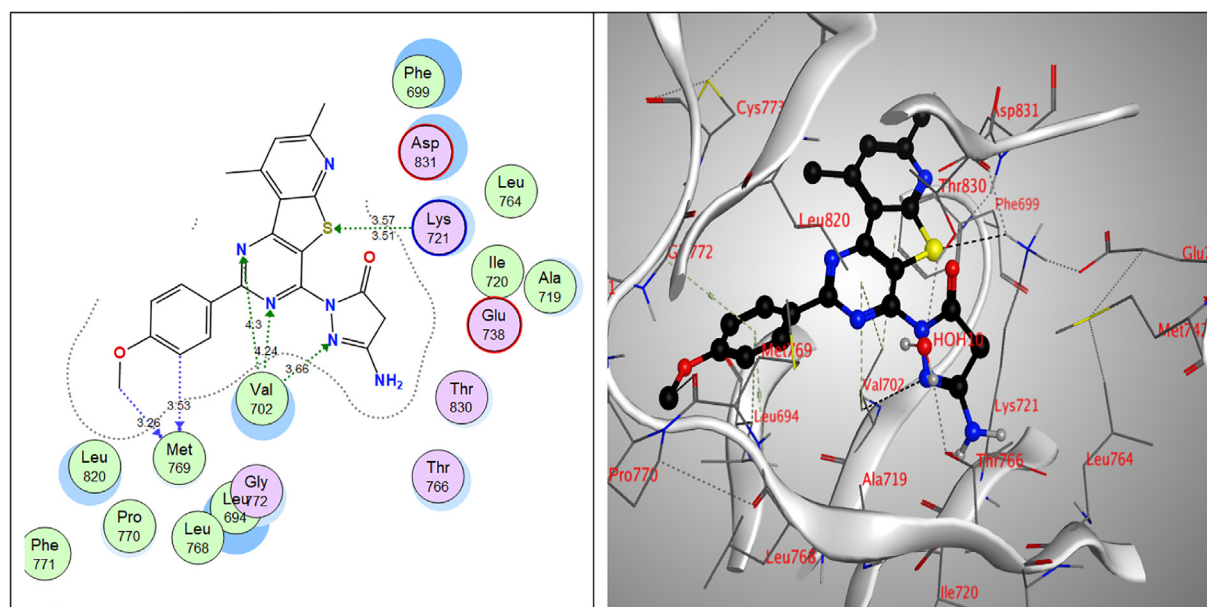
The Swiss ADME server provides a BOILED EGG chart to indicate the human intestinal absorption (white part), blood brain barrier penetration (the yellow part) and the probability of the tested compound to act as substrate for permeability glycoprotein (PGP) which is an efflux pump for many drugs \* (Sharom et al., 1997) (blue color if it's a possible substrate or red color if it's not). The results are summarized in (Fig. 9), compounds **7b** and **7c** were predicted to be not absorbed from the GIT but all others are expected to be of

good oral absorption which is indicated by their presence in the white area. All compounds are not present in the yellow area signifying the low probability to penetrate the blood–brain barrier (BBB) and not expected to cause CNS side effects. Finally, compounds **4a**, **6a** and **9a** are colored in red which means that they are anticipated to not be a substrate for PGP and not to be susceptible for efflux from the cells, while other derivatives are colored in blue which indicated their high probability to be substrates for PGP.

Eventually, we applied the Lipinski's rule of five (Giménez, et al., 2010) which predicts the drug-likeness and good oral bioavailability for the tested compounds. All compounds showed no violation in the applied four rules except compound **7b** which showed only one violation in having a log P value above 5, the rule states that no violation or even one violation indicates the expected good oral bioavailability. In a conclusion, although all compounds were parallel to Lipinski's rule of five but the radar chart excluded compound **7b** and the BOILED-Egg chart excluded both **7b** and **7c** compounds, so,

**Table 6** The docking results of the tested pyridothienopyrimidine compounds.

Compound	Docking score (kcal/mol)	Amino acids	Interacting groups	Type of interaction	Length
2b	-9.24	Leu768	N (Pyridine)	H-bond acceptor	3.78
		Cys751 (water)	O (C = O)	H-bond acceptor	2.86
		Thr766 (water)	O (C = O)	H-bond acceptor	2.86
		Thr830 (water)	O (C = O)	H-bond acceptor	2.86
4a	-9.56	Gln767	Cl	Halogen bond	3.74
		Met769	S	H-bond acceptor	3.65
6a	-13.31	Leu768	N (Pyridine)	H-bond acceptor	3.78
		Cys751 (water)	O (OH)	H-bond acceptor	2.97
		Thr766 (water)	O (OH)	H-bond acceptor	2.97
		Thr830 (water)	O (OH)	H-bond acceptor	2.97
7b	-12.53	Met742	N (Pyridine)	$\sigma$ -hole bond	3.99
		Thr830	S	$\sigma$ -hole bond	3.00
		Thr830	S (thiophene)	$\sigma$ -hole bond	4.08
		Asp831	NH	H-bond donor	2.90
7c	-13.56	Leu694	N (Pyrimidine)	H-bond acceptor	3.84
		Cys751 (water)	N (=N)	H-bond acceptor	2.83
		Thr766 (water)	N (=N)	H-bond acceptor	2.83
		Leu820	N (=N)	H-bond acceptor	3.50
		Thr830 (water)	N (=N)	H-bond acceptor	2.83
		Asp831	S	$\sigma$ -hole bond	4.09
9a	-13.82	Val702	N (Pyrazole)	H-bond acceptor	3.66
		Val702	N (Pyrimidine)	H-bond acceptor	4.24
		Val702	N (Pyrimidine)	H-bond acceptor	4.30
		Lys721	S	H-bond acceptor	3.51
		Met769	CH <sub>3</sub> (OCH <sub>3</sub> )	H-bond (non-classical)	3.26
		Met769	CH (Aromatic)	H-bond (non-classical)	3.53

**Fig. 5** 2D & 3D interactions of **9a** within EGFR<sup>WT</sup> active site.

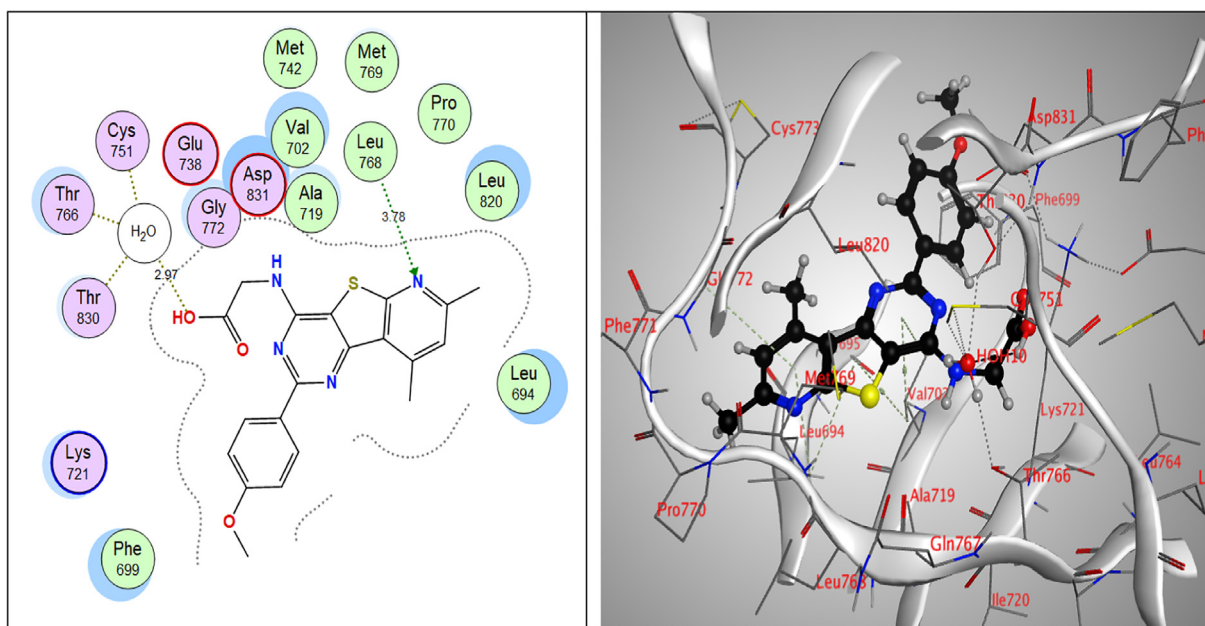


Fig. 6 2D & 3D interactions of 6a within EGFR<sup>WT</sup> active site.

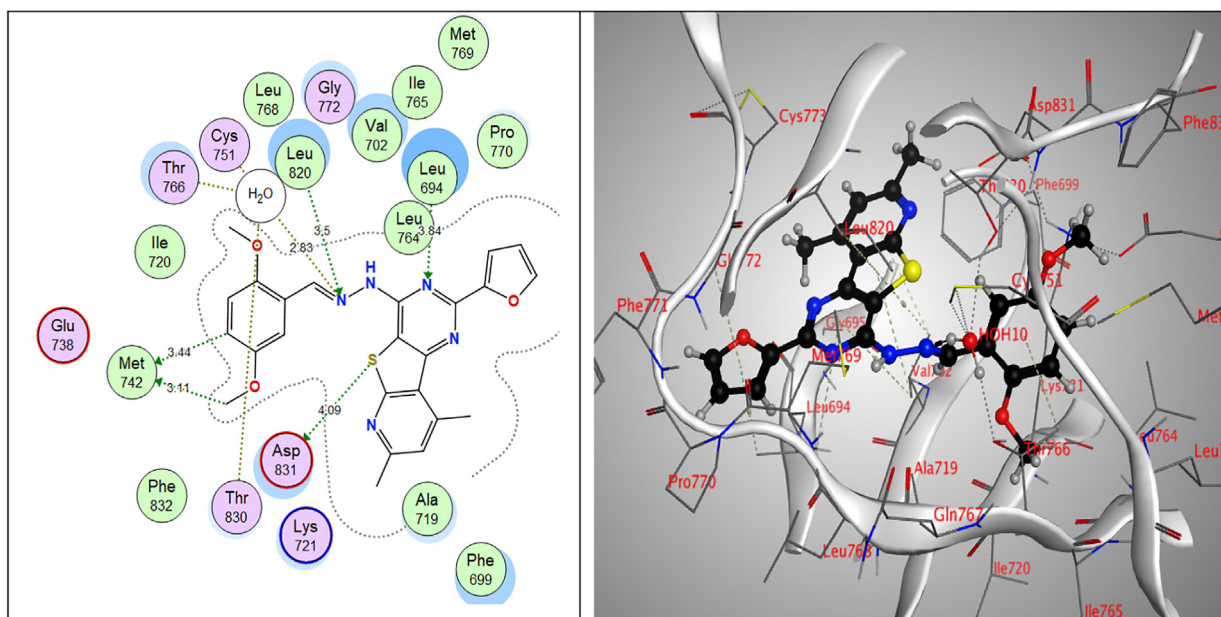
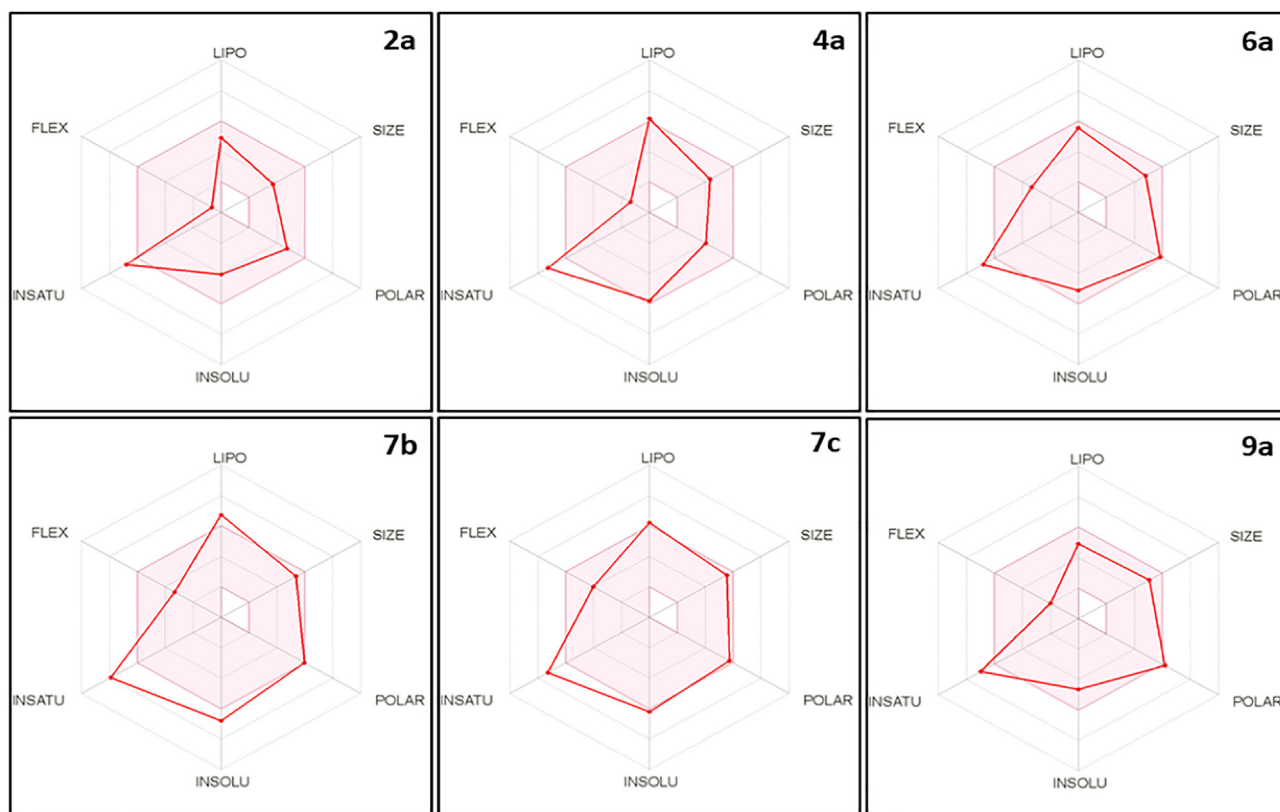
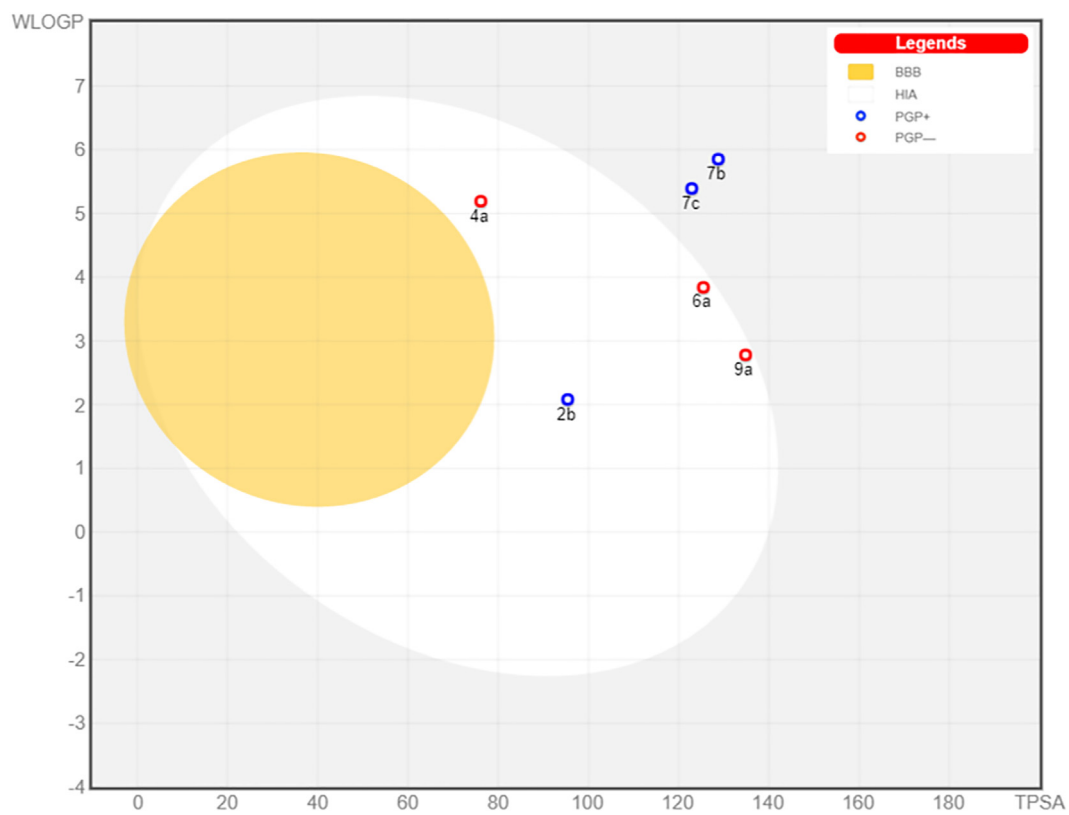


Fig. 7 2D & 3D interactions of 7c within EGFR<sup>WT</sup> active site.



**Fig. 8** The bioavailability radar chart for the tested compounds (the colored zone is the suitable physicochemical space for oral bioavailability).



**Fig. 9** BOILED-EGG chart for the tested compounds.

**Table 7** Drug-likeness of the tested compounds.

Compound NO.	Properties	Comment
<b>2b</b>	<ul style="list-style-type: none"> <li>• Log P = 2.51 (&lt;5)</li> <li>• Molecular weight = 299.35 g/mol (&lt;500)</li> <li>• No of H-bond donor groups (OHs + NHs) = 2 (<math>\leq 5</math>)</li> <li>• No of H-bond acceptor atoms (Os + Ns) = 5 (<math>\leq 10</math>)</li> </ul>	No violation
<b>4a</b>	<ul style="list-style-type: none"> <li>• Log P = 3.74 (&lt;5)</li> <li>• Molecular weight = 355.84 g/mol (&lt;500)</li> <li>• No of H-bond donor groups (OHs + NHs) = 0 (<math>\leq 5</math>)</li> <li>• No of H-bond acceptor atoms (Os + Ns) = 4 (<math>\leq 10</math>)</li> </ul>	No violation
<b>6a</b>	<ul style="list-style-type: none"> <li>• Log P = 3.15 (&lt;5)</li> <li>• Molecular weight = 394.45 g/mol (&lt;500)</li> <li>• No of H-bond donor groups (OHs + NHs) = 2 (<math>\leq 5</math>)</li> <li>• No of H-bond acceptor atoms (Os + Ns) = 7 (<math>\leq 10</math>)</li> </ul>	No violation
<b>7b</b>	<ul style="list-style-type: none"> <li>• Log P = 5.39 (&gt;5)</li> <li>• Molecular weight = 445.56 g/mol (&lt;500)</li> <li>• No of H-bond donor groups (OHs + NHs) = 1 (<math>\leq 5</math>)</li> <li>• No of H-bond acceptor atoms (Os + Ns) = 6 (<math>\leq 10</math>)</li> </ul>	One violation
<b>7c</b>	<ul style="list-style-type: none"> <li>• Log P = 4.63 (&lt;5)</li> <li>• Molecular weight = 459.52 g/mol (&lt;500)</li> <li>• No of H-bond donor groups (OHs + NHs) = 1 (<math>\leq 5</math>)</li> <li>• No of H-bond acceptor atoms (Os + Ns) = 8 (<math>\leq 10</math>)</li> </ul>	No violation
<b>9a</b>	<ul style="list-style-type: none"> <li>• Log P = 3.24 (&lt;5)</li> <li>• Molecular weight = 418.47 g/mol (&lt;500)</li> <li>• No of H-bond donor groups (OHs + NHs) = 2 (<math>\leq 5</math>)</li> <li>• No of H-bond acceptor atoms (Os + Ns) = 8 (<math>\leq 10</math>)</li> </ul>	No violation

both compounds need future further practical study to evaluate their actual oral bioavailability behavior. [Table 7](#) summarized the obtained data.

### 3. Conclusion

In summary, a new set of pyridothienopyrimidine compounds were designed, synthesized and evaluated for their dual antimicrobial and anticancer activities. All the new derivatives were evaluated as antimicrobial agents against a panel of bacterial and fungal strains. The MIC values of the compounds revealed that the 4-chloro analogue **4a**, amino acid derivatives **6a,c**, the Schiff's base **7c**, the tetracyclic derivative **8b** and the 4-pyrazolone derivatives **9a,b** exhibited the most potent antimicrobial activity compared with amoxicillin trihydrate and clotrimazole as standard antibacterial and antifungal drugs. Moreover, the *in vitro* cytotoxicity evaluation of the new derivatives against HepG2 and MCF-7 cell lines revealed the promising activity of the tested compounds against HepG2 cancer cells of IC<sub>50</sub> range; 1.80–48.70  $\mu$ M more than MCF-7 cells of IC<sub>50</sub> range; 10.80–80.61  $\mu$ M. The parent **2b**, **4a**, **6a**, the Schiff's bases **7b,c** and **9a** elicited the most potent cytotoxic activity against HepG-2 cell line of IC<sub>50</sub> values range; 1.80–5.63  $\mu$ M compared with doxorubicin as a positive control (IC<sub>50</sub>; 2.85  $\mu$ M) and IC<sub>50</sub> values ranging from 10.80 to 20.50  $\mu$ M compared with cisplatin as another positive control of IC<sub>50</sub> value 20.70  $\mu$ M. Further cytotoxic screening was carried out for the most potent compounds **2b**, **4a**, **6a**, **7b**, **7c** and **9a** against the normal cell line (WISH), which revealed their selective cytotoxicity against cancer cells and confirmed their promising safety profile. Additionally, the EGFR<sup>WT</sup> kinase inhibition assay for the latter derivatives showed the significant inhibitory activity of these compounds with IC<sub>50</sub> values range; 0.021–0.117  $\mu$ M in comparison to erlotinib as standard EGFR inhibitor of IC<sub>50</sub>; 0.027  $\mu$ M. Moreover, the 4-pyrazolone deriva-

tive **9a** exhibited more potent inhibitory activity than that of erlotinib with an IC<sub>50</sub> value of 0.021  $\mu$ M. While, a slight decrease in the activity was detected by **7c** and **6a**, which gave IC<sub>50</sub> values 0.032 and 0.046  $\mu$ M, respectively.

Furthermore, the most promising EGFR<sup>WT</sup> inhibitors **6a**, **7b**, **7c**, **9a** were also evaluated as inhibitors against the mutant forms EGFR<sup>L858R</sup> and EGFR<sup>T790M</sup> in comparison to erlotinib as a reference drug. The compound **9a** exhibited more potent suppression effect against both EGFR<sup>L858R</sup> and EGFR<sup>T790M</sup> than erlotinib of IC<sub>50</sub>s = 0.053, 0.081  $\mu$ M, respectively; IC<sub>50</sub> erlotinib; 0.041, 0.550  $\mu$ M, respectively followed by **7c** of IC<sub>50</sub>s = 0.252, 0.219  $\mu$ M, respectively. The molecular docking study confirmed that the binding modes of compounds **2b**, **4a**, **6a**, **7b**, **7c**, **9a** were consistent with the EGFR<sup>WT</sup> inhibitory activities. It was obvious that many of the target compounds have significant antimicrobial and/or anticancer activity and the most potent derivatives of dual activity were the 4-pyrazolone derivative **9a**, the glycine derivative **6a**, and the Schiff's base **7c**.

Based on the gained results, pyridothienopyrimidine scaffolds could be considered as a promising template for further developing and optimizing new analogues of more potent dual antimicrobial and anticancer agents via EGFR inhibitory effect.

### 4. Experimental

#### 4.1. Chemistry

The general information about the instruments utilized in the determination of the melting points, spectral data (IR, <sup>1</sup>H NMR, <sup>13</sup>C NMR, and Mass), and the elemental analysis of the target compounds are mentioned in detail in the [Supplementary material](#). The starting compound 3-amino-4,6-dimethylthieno[2,3-*b*]pyridine-2-carboxamide (**1**) was prepared as the reported method (Youssefyeh, et al., 1984)

#### 4.1.1. Synthesis of 2,3-dihydropyridothienopyrimidin-4(1H)-ones 2a,b

A mixture solution of compound **1** (0.02 mol) and the appropriate aldehyde namely; 4-methoxybenzaldehyde or furan-2-carbaldehyde (0.02 mol) in glacial acetic acid (30 mL) was refluxed for 8 h. After reaction completion, the solvent was evaporated till dryness under reduced pressure and the obtained precipitate was filtered, washed several times with water, and recrystallized from ethanol to give compounds **2a,b**.

4.1.1.1. 2-(4-Methoxyphenyl)-7,9-dimethyl-2,3-dihydropyrido[3',2':4,5]thieno[3,2-d]pyrimidin-4(1H)-one (**2a**). Yield 82%, brownish powder, m.p. 210 °C; IR (KBr,  $\nu_{\max}/\text{cm}^{-1}$ ): 3424, 3254 (2NH), 3029 (CH-aromatic), 2958, 2836 (CH-aliphatic), 1656 (C = O);  $^1\text{H}$  NMR (400 MHz, DMSO  $d_6$ ,  $\delta$  ppm): 2.49 (s, 3H, CH<sub>3</sub>), 2.70 (s, 3H, CH<sub>3</sub>), 3.71 (s, 3H, OCH<sub>3</sub>), 5.81 (s, 1H, CH-pyrimidinone), 6.91 (d, 2H,  $J$  = 8.4 Hz, Ar-H), 7.02 (s, 1H, NH, D<sub>2</sub>O exchangeable), 7.06 (s, 1H, Ar-H), 7.44 (d, 2H,  $J$  = 8.4 Hz, Ar-H), 8.32 (s, 1H, NH, D<sub>2</sub>O exchangeable);  $^{13}\text{C}$  NMR (100 MHz, DMSO  $d_6$ ,  $\delta$  ppm): 19.73, 24.38 (2CH<sub>3</sub>), 55.63 (OCH<sub>3</sub>), 66.13 (CH-pyrimidinone), 114.07, 122.12, 123.01, 128.27, 128.58, 133.84, 137.61, 145.23, 145.33, 159.05, 159.86 (Ar-C), 162.11 (C = O); MS,  $m/z$  (%): 339 (M<sup>+</sup>, 37); Anal. Calc. for C<sub>18</sub>H<sub>17</sub>N<sub>3</sub>O<sub>2</sub>S (339.41): Calcd. C, 63.70; H, 5.05; N, 12.38; S, 9.45; found C, 63.42, H, 4.88; N, 12.10; S, 9.14.

4.1.1.2. 2-(Furan-2-yl)-7,9-dimethyl-2,3-dihydropyrido[3',2':4,5]thieno[3,2-d]pyrimidin-4(1H)-one (**2b**). Yield 76%, brownish powder, m.p. 245 °C; IR (KBr,  $\nu_{\max}/\text{cm}^{-1}$ ): 3304, 3225 (2NH), 3029 (CH-aromatic), 2975, 2931 (CH-aliphatic), 1660 (C = O);  $^1\text{H}$  NMR (400 MHz, DMSO  $d_6$ ,  $\delta$  ppm): 2.51 (s, 3H, CH<sub>3</sub>), 2.68 (s, 3H, CH<sub>3</sub>), 5.90 (s, 1H, CH-pyrimidinone), 6.31–6.37 (m, 2H, Ar-H), 7.06 (s, 1H, Ar-H), 7.16 (s, 1H, NH, D<sub>2</sub>O exchangeable), 7.61 (s, 1H, Ar-H), 8.35 (s, 1H, NH, D<sub>2</sub>O exchangeable);  $^{13}\text{C}$  NMR (100 MHz, DMSO  $d_6$ ,  $\delta$  ppm): 19.64, 24.33 (2CH<sub>3</sub>), 61.41 (CH-pyrimidinone), 107.52, 108.00, 110.81, 122.05, 123.02, 143.35, 144.59, 145.08, 154.25, 159.98, 161.62 (Ar-C), 161.75 (C = O); MS,  $m/z$  (%): 299 (M<sup>+</sup>, 25); Anal. Calc. for C<sub>15</sub>H<sub>13</sub>N<sub>3</sub>O<sub>2</sub>S (299.35): Calcd. C, 60.19; H, 4.38; N, 14.04; S, 10.71; found C, 59.91; H, 4.13; N, 13.87; S, 10.42.

#### 4.1.2. Synthesis of pyridothienopyrimidin-4(3H)-one derivatives 3a,b

A mixture of compounds **2a,b** (0.01 mol), and benzoquinone (0.01 mol) in absolute ethanol (50 mL) was refluxed for 9 h. The solid formed was collected by filtration, washed with hot water, and recrystallized from DMF/EtOH to give compounds **3a,b**.

4.1.2.1. 2-(4-Methoxyphenyl)-7,9-dimethylpyrido[3',2':4,5]thieno[3,2-d]pyrimidin-4(3H)-one (**3a**). Yield 66 %, greyish powder, m.p. 340 °C; IR (KBr,  $\nu_{\max}/\text{cm}^{-1}$ ): 3435 (NH), 2921 (CH-aliphatic), 1668 (C = O);  $^1\text{H}$  NMR (400 MHz, DMSO  $d_6$ ,  $\delta$  ppm): 2.54 (s, 3H, CH<sub>3</sub>), 2.91 (s, 3H, CH<sub>3</sub>), 3.85 (s, 3H, OCH<sub>3</sub>), 7.07 (d, 2H,  $J$  = 8.0 Hz, Ar-H), 7.19 (s, 1H, Ar-H), 8.17 (d, 2H,  $J$  = 8.0 Hz, Ar-H), 12.83 (s, 1H, NH, D<sub>2</sub>O exchangeable);  $^{13}\text{C}$  NMR (100 MHz, DMSO  $d_6$ ,  $\delta$

ppm): 19.43, 24.51 (2CH<sub>3</sub>), 56.09 (OCH<sub>3</sub>), 114.52, 122.21, 123.33, 127.70, 130.57, 145.41, 153.21, 154.56, 159.30, 159.88, 160.16 (Ar-C), 162.59 (C = O); MS,  $m/z$  (%): 337 (M<sup>+</sup>, 48); Anal. Calc. for C<sub>18</sub>H<sub>15</sub>N<sub>3</sub>O<sub>2</sub>S (337.40): Calcd. C, 64.08; H, 4.48; N, 12.45; S, 9.50; found C, 64.23; H, 4.26; N, 12.69; S, 9.31.

4.1.2.2. 2-(Furan-2-yl)-7,9-dimethylpyrido[3',2':4,5]thieno[3,2-d]pyrimidin-4(3H)-one (**3b**). Yield 62%, greyish powder, m.p. 350–351 °C; IR (KBr,  $\nu_{\max}/\text{cm}^{-1}$ ): 3376 (NH), 3008 (CH-aromatic), 2952 (CH-aliphatic), 1658 (C = O);  $^1\text{H}$  NMR (400 MHz, DMSO  $d_6$ ,  $\delta$  ppm): 2.46 (s, 3H, CH<sub>3</sub>), 2.82 (s, 3H, CH<sub>3</sub>), 7.08–8.01 (m, 4H, Ar-H), 13.0 (s, 1H, NH, D<sub>2</sub>O exchangeable);  $^{13}\text{C}$  NMR (100 MHz, DMSO  $d_6$ ,  $\delta$  ppm): 19.11, 24.51 (2CH<sub>3</sub>), 113.18, 115.14, 121.29, 124.58, 134.80, 145.59, 147.16, 147.21, 150.03, 152.05, 159.92, 160.13 (Ar-C), 162.09 (C = O); MS,  $m/z$  (%): 297 (M<sup>+</sup>, 26); Anal. Calc. for C<sub>15</sub>H<sub>11</sub>N<sub>3</sub>O<sub>2</sub>S (297.33): Calcd. C, 60.59; H, 3.73; N, 14.13; S, 10.78; found C, 60.32; H, 3.48; N, 14.01; S, 10.5.

#### 4.1.3. Synthesis of 4-chloropyridothienopyrimidine derivatives 4a,b

A mixture of compounds **3a,b** (5 mmol), phosphorus oxychloride (15 mL), and phosphorous pentachloride (5 mmol) was heated on a boiling water bath for 12 h. After the reaction completion, the mixture solution was left to cool then poured gradually with continuous stirring onto crushed ice. The obtained solid was filtered, washed with water, and recrystallized from DMF to give the corresponding chloro derivatives **4a,b**.

4.1.3.1. 4-chloro-2-(4-methoxyphenyl)-7,9-dimethylpyrido[3',2':4,5]thieno[3,2-d]pyrimidine (**4a**). Yield 87%, brownish powder, m.p. 270 °C; IR (KBr,  $\nu_{\max}/\text{cm}^{-1}$ ): 3021 (CH-aromatic), 2991 (CH-aliphatic), 1620 (C = N);  $^1\text{H}$  NMR (400 MHz, DMSO  $d_6$ ,  $\delta$  ppm): 2.47 (s, 3H, CH<sub>3</sub>), 2.77 (s, 3H, CH<sub>3</sub>), 3.77 (s, 3H, OCH<sub>3</sub>), 6.92 (d, 2H,  $J$  = 10.4 Hz, Ar-H), 7.13 (s, 1H, Ar-H), 8.09 (d, 2H,  $J$  = 10.4 Hz, Ar-H);  $^{13}\text{C}$  NMR (100 MHz, DMSO  $d_6$ ,  $\delta$  ppm): 19.71, 24.35 (2CH<sub>3</sub>), 55.61 (OCH<sub>3</sub>), 114.73, 121.22, 122.95, 123.81, 127.15, 129.90, 145.57, 154.09, 159.94, 160.89, 161.09, 161.89 (Ar-C); MS,  $m/z$  (%): 355 (M<sup>+</sup>, 63); Anal. Calc. for C<sub>18</sub>H<sub>14</sub>ClN<sub>3</sub>OS (355.84): Calcd. C, 60.76; H, 3.97; N, 11.81; S, 9.01; found C, 60.34; H, 3.72; N, 12.11; S, 8.74.

4.1.3.2. 4-chloro-2-(furan-2-yl)-7,9-dimethylpyrido[3',2':4,5]thieno[3,2-d]pyrimidine (**4b**). Yield 80%, greyish powder, m.p. 261 °C; IR (KBr,  $\nu_{\max}/\text{cm}^{-1}$ ): 3107 (CH-aromatic), 2919 (CH-aliphatic), 1618 (C = N);  $^1\text{H}$  NMR (400 MHz, DMSO  $d_6$ ,  $\delta$  ppm): 2.50 (s, 3H, CH<sub>3</sub>), 2.77 (s, 3H, CH<sub>3</sub>), 6.66 (t, 1H, Ar-H), 7.07 (s, 1H, Ar-H), 7.19 (d, 1H,  $J$  = 9.6 Hz, Ar-H), 7.93 (d, 1H,  $J$  = 12.4 Hz, Ar-H);  $^{13}\text{C}$  NMR (100 MHz, DMSO  $d_6$ ,  $\delta$  ppm): 19.09, 24.52 (2CH<sub>3</sub>), 113.08, 114.63, 122.54, 123.50, 125.59, 145.70, 148.11, 150.88, 153.39, 153.50, 159.87, 162.18, 162.24 (Ar-C); MS,  $m/z$  (%): 315 (M<sup>+</sup>, 25); Anal. Calc. for C<sub>15</sub>H<sub>10</sub>ClN<sub>3</sub>OS (315.78): Calcd. C, 57.05; H, 3.19; N, 13.31; S, 10.15; found C, 56.78; H, 2.89; N, 13.53; S, 9.88.

#### 4.1.4. Synthesis of 4-hydrazineylpyrido[3',2':4,5]thieno[3,2-d]pyrimidine derivatives 5a,b

A mixture of the chloro derivatives **4a,b** (5 mmol), and hydrazine hydrate (20 mmol) in ethanol (70 mL) was refluxed for 4 h. After the reaction completion, the excess solvent was evaporated till dryness under reduced pressure. Then the obtained precipitate was washed with water, collected by filtration, and recrystallized from EtOH/H<sub>2</sub>O to give the corresponding target compounds **5a,b**.

4.1.4.1. 4-Hydrazineyl-2-(4-methoxyphenyl)-7,9-dimethylpyrido[3',2':4,5]thieno[3,2-d]pyrimidine (5a). Yield 88%, yellowish powder, m.p. 220 °C; IR (KBr,  $\nu_{\max}/\text{cm}^{-1}$ ): 3380, 3335 (NH, NH<sub>2</sub>), 3086 (CH-aromatic), 2918, 2832 (CH-aliphatic), 1622 (C = N); <sup>1</sup>H NMR (400 MHz, DMSO *d*<sub>6</sub>,  $\delta$  ppm): 2.51 (s, 3H, CH<sub>3</sub>), 2.61 (s, 3H, CH<sub>3</sub>), 3.84 (s, 3H, OCH<sub>3</sub>), 4.94 (s, 2H, NH<sub>2</sub>, D<sub>2</sub>O exchangeable), 7.05 (d, 2H, *J* = 8.7 Hz, Ar-H), 7.22 (s, 1H, Ar-H), 8.37 (d, 2H, *J* = 8.6 Hz, Ar-H), 9.02 (s, 1H, NH, D<sub>2</sub>O exchangeable); <sup>13</sup>C NMR (100 MHz, DMSO *d*<sub>6</sub>,  $\delta$  ppm): 19.90, 24.55 (2CH<sub>3</sub>), 55.70 (OCH<sub>3</sub>), 114.12, 116.29, 122.44, 123.47, 129.54, 131.12, 135.03, 145.21, 146.47, 158.22, 159.60, 159.78, 161.35 (Ar-C); MS, *m/z* (%): 351 (M<sup>+</sup>, 58); Anal. Calc. for C<sub>18</sub>H<sub>17</sub>N<sub>5</sub>OS (351.43): Calcd. C, 61.52; H, 4.88; N, 19.93; S, 9.12; found C, 61.24; H, 4.65; N, 19.68; S, 8.83.

4.1.4.2. 2-(Furan-2-yl)-4-hydrazineyl-7,9-dimethylpyrido[3',2':4,5]thieno[3,2-d]pyrimidine (5b). Yield 89%, yellowish powder, m.p. 218 °C; IR (KBr,  $\nu_{\max}/\text{cm}^{-1}$ ): 3324, 3288 (NH, NH<sub>2</sub>), 3109 (CH-aromatic), 2921 (CH-aliphatic); <sup>1</sup>H NMR (400 MHz, DMSO *d*<sub>6</sub>,  $\delta$  ppm): 2.58 (s, 3H, CH<sub>3</sub>), 2.98 (s, 3H, CH<sub>3</sub>), 4.94 (s, 2H, NH<sub>2</sub>, D<sub>2</sub>O exchangeable), 6.65–7.90 (m, 4H, Ar-H), 9.25 (s, 1H, NH, D<sub>2</sub>O exchangeable); <sup>13</sup>C NMR (100 MHz, DMSO *d*<sub>6</sub>,  $\delta$  ppm): 19.23, 24.51 (2CH<sub>3</sub>), 110.40, 114.64, 122.41, 123.45, 125.53, 145.42, 147.20, 150.47, 153.50, 159.82, 160.01, 161.36, 163.08 (Ar-C); MS, *m/z* (%): 311 (M<sup>+</sup>, 100); Anal. Calc. for C<sub>15</sub>H<sub>13</sub>N<sub>5</sub>OS (311.36): Calcd. C, 57.86; H, 4.21; N, 22.49; S, 10.30; found C, 57.59; H, 3.99; N, 22.21; S, 10.03.

#### 4.1.5. Synthesis of (pyridothienopyrimidin-4-yl) amino acid derivatives 6a-c

A mixture of the chloro derivatives **4a,b** (1 mmol), and the appropriate amino acids (1 mmol), namely; glycine, valine, and alanine in DMSO (20 mL) containing anhydrous sodium carbonate (0.2 g) was stirred on a water bath at 80 °C for 6 h. Then, the reaction solution was poured onto ice/water and the reaction medium was neutralized with dil. HCl (pH; 7). The formed precipitate was collected by filtration, washed with water, and recrystallized from dioxane to give the corresponding compounds **6a-c**.

4.1.5.1. 2-(4-Methoxyphenyl)-7,9-dimethylpyrido[3',2':4,5]thieno[3,2-d]pyrimidin-4-ylglycine (6a). Yield 61%, brownish powder, m.p. 256 °C, IR (KBr,  $\nu_{\max}/\text{cm}^{-1}$ ): 3395 (broad, OH), 3344 (NH), 3073 (CH-aromatic), 2957, 2920 (CH-aliphatic), 1670 (C = O); <sup>1</sup>H NMR (400 MHz, DMSO *d*<sub>6</sub>,  $\delta$  ppm): 2.47 (s, 3H, CH<sub>3</sub>), 2.87 (s, 3H, CH<sub>3</sub>), 3.75 (s, 3H, OCH<sub>3</sub>), 4.11 (s, 2H, -NH-CH<sub>2</sub>), 6.99 (s, 1H, Ar-H), 7.06 (d, 2H, *J* = 8.4 Hz, Ar-H), 7.47 (1H, NH, D<sub>2</sub>O exchangeable), 8.21 (d, 2H, *J* = 8.5 Hz, Ar-H), 12.23 (s, 1H, OH, D<sub>2</sub>O

exchangeable); <sup>13</sup>C NMR (100 MHz, DMSO *d*<sub>6</sub>,  $\delta$  ppm): 19.51, 24.45 (2CH<sub>3</sub>), 44.86 (-NH-CH<sub>2</sub>), 55.63 (OCH<sub>3</sub>), 109.81, 114.87, 122.52, 123.50, 129.67, 131.33, 138.42, 145.41, 146.94, 148.22, 157.08, 159.70, 161.56 (Ar-C), 176.14 (C = O); MS, *m/z* (%): 394 (M<sup>+</sup>, 52); Anal. Calc. for C<sub>20</sub>H<sub>18</sub>N<sub>4</sub>O<sub>3</sub>S (394.45): Calcd. C 60.90; H, 4.60; N, 14.20; S, 8.13; found C, 60.63; H, 4.35; N, 13.92; S, 7.84.

4.1.5.2. 2-(4-Methoxyphenyl)-7,9-dimethylpyrido[3',2':4,5]thieno[3,2-d]pyrimidin-4-ylvaline (6b). Yield 63%, brownish powder, m.p. 244 °C; IR (KBr,  $\nu_{\max}/\text{cm}^{-1}$ ): 3400 (broad, OH), 3323 (NH), 3090 (CH-aromatic), 2960, 2850 (CH-aliphatic), 1676 (C = O); <sup>1</sup>H NMR (400 MHz, DMSO *d*<sub>6</sub>,  $\delta$  ppm): 0.99 (d, 6H, *J* = 8.4 Hz, -CH-(CH<sub>3</sub>)<sub>2</sub>), 1.90 (m, 1H, -CH-(CH<sub>3</sub>)<sub>2</sub>), 2.44 (s, 3H, CH<sub>3</sub>), 2.70 (s, 3H, CH<sub>3</sub>), 3.04 (d, 1H, *J* = 6.8 Hz, -NH-CH), 3.85 (s, 3H, OCH<sub>3</sub>), 7.16 (d, 2H, *J* = 12.8 Hz, Ar-H), 7.32 (s, 1H, Ar-H), 7.59 (s, 1H, NH, D<sub>2</sub>O exchangeable), 8.30 (d, 2H, *J* = 12.8 Hz, Ar-H), 12.81 (s, 1H, OH, D<sub>2</sub>O exchangeable); <sup>13</sup>C NMR (100 MHz, DMSO *d*<sub>6</sub>,  $\delta$  ppm): 19.30, 19.59, 24.49 (4CH<sub>3</sub>), 45.79 (-CH-(CH<sub>3</sub>)<sub>2</sub>), 55.60 (OCH<sub>3</sub>), 67.97 (-NH-CH<sub>2</sub>), 105.30, 114.27, 122.45, 123.48, 131.20, 137.61, 140.45, 143.80, 145.47, 159.83, 161.40, 164.67 (Ar-C), 176.73 (C = O); MS, *m/z* (%): 436 (M<sup>+</sup>, 39); Anal. Calc. for C<sub>23</sub>H<sub>24</sub>N<sub>4</sub>O<sub>3</sub>S (436.53): Calcd. C, 63.28; H, 5.54; N, 12.83; S, 7.34; found C, 63.54; H, 5.25; N, 13.06; S, 7.59.

4.1.5.3. 2-(Furan-2-yl)-7,9-dimethylpyrido[3',2':4,5]thieno[3,2-d]pyrimidin-4-ylalanine (6c). Yield 62%, brownish powder, m.p. 197 °C; IR (KBr,  $\nu_{\max}/\text{cm}^{-1}$ ): 3393 (broad, OH), 3312 (NH), 3061 (CH-aromatic), 2919, 2852 (CH-aliphatic), 1671 (C = O); <sup>1</sup>H NMR (400 MHz, DMSO *d*<sub>6</sub>,  $\delta$  ppm): 1.52 (d, 3H, *J* = 5.2 Hz, -CH-CH<sub>3</sub>), 2.83 (s, 3H, CH<sub>3</sub>), 2.90 (s, 3H, CH<sub>3</sub>), 3.34 (m, 1H, -NH-CH), 6.69 (s, 1H, NH, D<sub>2</sub>O exchangeable), 6.76–8.22 (m, 4H, Ar-H), 12.83 (s, 1H, OH, D<sub>2</sub>O exchangeable); <sup>13</sup>C NMR (100 MHz, DMSO *d*<sub>6</sub>,  $\delta$  ppm): 19.52, 20.17, 24.45 (3CH<sub>3</sub>), 48.82 (-HN-CH), 100.21, 114.13, 122.43, 123.55, 131.56, 135.62, 141.33, 143.91, 145.48, 159.80, 162.50, 165.03 (Ar-C), 176.75 (C = O); MS, *m/z* (%): 368 (M<sup>+</sup>, 46); Anal. Calc. for C<sub>18</sub>H<sub>16</sub>N<sub>4</sub>O<sub>3</sub>S (368.41): Calcd. C, 58.68; H, 4.38; N, 15.21; S, 8.70; found C, 58.34; H, 4.74; N, 15.01; S, 8.52.

#### 4.1.6. Synthesis of 4-(2-(Arylidene)hydrazineyl)pyridothienopyrimidine derivatives 7a-c

A mixture of the hydrazide compounds **5a,b** (1 mmol) and different aldehydes, namely; 4-methylbenzaldehyde, 2,5-dimethoxybenzaldehyde, and thiophene-2-carbaldehyde (1 mmol) in ethanol/glacial acetic acid solution (1:1, 20 mL) was refluxed for 12 h. The reaction solution was concentrated and poured onto cold water and the formed solid was filtered, washed with water, and crystallized from ethanol to give the corresponding compounds **7a-c**.

4.1.6.1. 2-(4-Methoxyphenyl)-7,9-dimethyl-4-(2-(4-methylbenzylidene)hydrazineyl)pyrido[3',2':4,5]thieno[3,2-d]pyrimidine (7a). Yield 66%, yellowish powder, m.p. 125 °C; IR (KBr,  $\nu_{\max}/\text{cm}^{-1}$ ): 3303, 3186 (NH), 3084 (CH-aromatic), 2954, 2919 (CH-aliphatic), 1632 (C = N); <sup>1</sup>H NMR (400 MHz, DMSO *d*<sub>6</sub>,  $\delta$  ppm): 2.38 (s, 3H, CH<sub>3</sub>), 2.62 (s, 3H, CH<sub>3</sub>), 3.07 (s, 3H, CH<sub>3</sub>), 3.85 (s, 3H, OCH<sub>3</sub>), 7.05–8.23 (m, 9H,

Ar-H), 8.43 (s, 1H, -N = CH), 12.09 (s, 1H, NH, D<sub>2</sub>O exchangeable); <sup>13</sup>C NMR (100 MHz, DMSO *d*<sub>6</sub>, δ ppm): 19.93, 21.60, 24.46 (3CH<sub>3</sub>), 55.61 (OCH<sub>3</sub>), 108.03, 114.45, 114.62, 122.25, 123.72, 126.81, 127.12, 129.50, 129.90, 132.37, 139.45, 145.51, 146.85, 156.30, 159.04, 159.96, 161.30, 167.98 (Ar-C); MS, *m/z* (%): 453 (M<sup>+</sup>, 38); Anal. Calc. for C<sub>26</sub>H<sub>23</sub>N<sub>5</sub>OS (453.56): Calcd. C, 68.85; H, 5.11; N, 15.44; S, 7.07; found C, 68.55; H, 4.86; N, 15.18; S, 7.32.

4.1.6.2. 2-(4-Methoxyphenyl)-7,9-dimethyl-4-(2-(thiophen-2-ylmethylene)hydrazineyl)pyrido [3',2':4,5]thieno[3,2-d]pyrimidine (7b). Yield 68%, brownish powder, m.p. 116 °C; IR (KBr, *v*<sub>max</sub>/cm<sup>-1</sup>): 3341, 3155 (NH), 3099 (CH-aromatic), 2956, 2927 (CH-aliphatic), 1608 (C = N); <sup>1</sup>H NMR (400 MHz, DMSO *d*<sub>6</sub>, δ ppm): 2.58 (s, 3H, CH<sub>3</sub>), 2.99 (s, 3H, CH<sub>3</sub>), 3.88 (s, 3H, OCH<sub>3</sub>), 7.03–8.30 (m, 8H, Ar-H), 8.77 (s, 1H, -N = CH), 12.01 (s, 1H, NH, D<sub>2</sub>O exchangeable); <sup>13</sup>C NMR (100 MHz, DMSO *d*<sub>6</sub>, δ ppm): 19.91, 24.54 (2CH<sub>3</sub>), 56.07 (OCH<sub>3</sub>), 108.90, 114.52, 114.94, 122.30, 123.82, 127.64, 128.35, 129.51, 131.20, 132.43, 145.47, 146.82, 157.31, 159.16, 159.93, 160.30, 162.21, 166.93 (Ar-C); MS, *m/z* (%): 445 (M<sup>+</sup>, 40); Anal. Calc. for C<sub>23</sub>H<sub>19</sub>N<sub>5</sub>OS<sub>2</sub> (445.56): Calcd. C, 62.00; H, 4.30; N, 15.72; S, 14.39; found C, 61.73; H, 4.05; N, 15.44; S, 14.11.

4.1.6.3. 4-(2-(2,5-Dimethoxybenzylidene)hydrazineyl)-2-(furan-2-yl)-7,9-dimethylpyrido [3',2':4,5]thieno[3,2-d]pyrimidine (7c). Yield 68%, Yellowish powder, m.p. 126 °C; IR (KBr, *v*<sub>max</sub>/cm<sup>-1</sup>): 3253, 3143 (NH), 3105 (CH-aromatic), 2993, 2949 (CH-aliphatic), 1613 (CH = N); <sup>1</sup>H NMR (DMSO *d*<sub>6</sub>, δ ppm): 2.50 (s, 3H, CH<sub>3</sub>), 2.89 (s, 3H, CH<sub>3</sub>), 3.79 (s, 3H, OCH<sub>3</sub>), 3.83 (s, 3H, OCH<sub>3</sub>), 6.63–7.83 (m, 7H, Ar-H), 8.39 (s, 1H, -CH = N), 12.20 (s, 1H, NH, D<sub>2</sub>O exchangeable); <sup>13</sup>C NMR (100 MHz, DMSO *d*<sub>6</sub>, δ ppm): 19.66, 24.50 (2CH<sub>3</sub>), 55.73, 56.54 (2OCH<sub>3</sub>), 108.76, 110.54, 112.34, 112.47, 113.37, 116.39, 122.57, 122.91, 123.57, 138.34, 145.44, 146.82, 152.15, 152.86, 153.18, 153.64, 156.44, 157.20, 160.02, 164.50 (Ar-C, -CH = N); MS, *m/z* (%): 459 (M<sup>+</sup>, 60); Anal. Calc. for C<sub>24</sub>H<sub>21</sub>N<sub>5</sub>O<sub>3</sub>S (459.52): Calcd. C, 62.73; H, 4.61; N, 15.24; S, 6.98; found C, 62.51; H, 4.34; N, 15.01; S, 7.21.

#### 4.1.7. Synthesis of pyridothienotriazolopyrimidine derivatives 8a,b

A solution of compound **5a,b** (2 mmol) in formic acid (10 mL) was refluxed for 6 h. The excess solvent was evaporated under reduced pressure till dryness. Then the obtained solid was washed with water, collected by filtration, and recrystallized from DMF/H<sub>2</sub>O to give the corresponding compounds **8a,b**.

4.1.7.1. 5-(4-Methoxyphenyl)-7,9-dimethylpyrido [3',2':4,5]thieno[2,3-*e*] [1,2,4] triazolo[4,3-*c*] pyrimidine (8a). Yield 79%, brown solid, m.p. 240 °C; IR (KBr, *v*<sub>max</sub>/cm<sup>-1</sup>): 3098 (CH-aromatic), 2943, 2863 (CH-aliphatic), 1619 (C = N); <sup>1</sup>H NMR (400 MHz, DMSO *d*<sub>6</sub>, δ ppm): 2.54 (s, 3H, CH<sub>3</sub>), 2.81 (s, 3H, CH<sub>3</sub>), 3.88 (s, 3H, OCH<sub>3</sub>), 7.02 (d, 2H, *J* = 8.8 Hz, Ar -H), 7.22 (s, 1H, Ar-H), 8.01 (d, 2H, *J* = 8.8 Hz, Ar-H), 9.51 (s, 1H, 1,2,4-triazole-H<sub>3</sub>); <sup>13</sup>C NMR (100 MHz, DMSO *d*<sub>6</sub>, δ ppm): 19.41, 24.45 (2CH<sub>3</sub>), 56.16 (OCH<sub>3</sub>), 114.20, 122.44, 123.61, 129.87, 129.51, 131.27, 136.80, 137.91, 142.73, 145.52, 159.92, 162.43 (Ar-C); MS, *m/z* (%): 361 (M<sup>+</sup>, 33); Anal. Calc. for C<sub>19</sub>H<sub>15</sub>N<sub>5</sub>O

(361.42): Calcd. C, 63.14; H, 4.18; N, 19.38; S, 8.87; found C, 62.88; H, 3.89; N, 19.11; S, 8.58.

4.1.7.2. 5-(Furan-2-yl)-7,9-dimethylpyrido[3',2':4,5]thieno [2,3-*e*][1,2,4]triazolo[4,3-*c*] pyrimidine (8b). Yield 75%, brown solid, m.p. 275 °C; IR (KBr, *v*<sub>max</sub>/cm<sup>-1</sup>): 3103 (CH-aromatic), 2919, 2851 (CH-aliphatic), 1620 (C = N); <sup>1</sup>H NMR (400 MHz, DMSO *d*<sub>6</sub>, δ ppm): 2.45 (s, 3H, CH<sub>3</sub>), 2.66 (s, 3H, CH<sub>3</sub>), 6.86–8.11 (m, 4H, Ar-H), 9.74 (s, 1H, 1,2,4-triazole-H<sub>3</sub>); <sup>13</sup>C NMR (100 MHz, DMSO *d*<sub>6</sub>, δ ppm): 19.20, 24.57 (2CH<sub>3</sub>), 112.20, 115.06, 122.40, 123.84, 129.50, 132.22, 138.50, 142.71, 143.66, 145.50, 154.73, 159.90, 161.23, 165.41 (Ar-C); MS, *m/z* (%): 321 (M<sup>+</sup>, 45); Anal. Calc. for C<sub>16</sub>H<sub>11</sub>N<sub>5</sub>OS (321.36): Calcd. C, 59.80; H, 3.45; N, 21.79; S, 9.98; found C, 59.53; H, 3.23; N, 21.51; S, 9.69.

#### 4.1.8. Synthesis of 5-amino-2-(pyridothienopyrimidin-4-yl)-2,4-dihydro-3H-pyrazol-3-one derivatives 9a,b

A mixture of compound **5a,b** (1 mmol), and ethyl cyanoacetate (1 mmol) in ethanol/glacial acetic acid solution (3:1; 20 mL) was refluxed for 10h. The reaction solution was evaporated under reduced pressure till dryness, then treated with water. The solid obtained was filtered, washed with water, and recrystallized from ethanol to give the corresponding compounds **9a,b**.

4.1.8.1. 5-Amino-2-(2-(4-methoxyphenyl)-7,9-dimethylpyrido [3',2':4,5] thieno[3,2-d]pyrimidin-4-yl)-2,4-dihydro-3H-pyrazol-3-one (9a). Yield 85%, Yellowish powder, m.p. 249 °C; IR (KBr, *v*<sub>max</sub>/cm<sup>-1</sup>): 3212 (NH<sub>2</sub>), 3092 (CH-aromatic), 2933, 2843 (CH-aliphatic), 1695 (C = O); <sup>1</sup>H NMR (400 MHz, DMSO *d*<sub>6</sub>, δ ppm): 2.60 (s, 3H, CH<sub>3</sub>), 2.97 (s, 3H, CH<sub>3</sub>), 3.06 (s, 2H, pyrazolone-CH<sub>2</sub>), 3.85 (s, 3H, OCH<sub>3</sub>), 7.08–8.45 (m, 5H, Ar-H), 9.58 (s, 2H, NH<sub>2</sub>, D<sub>2</sub>O exchangeable); <sup>13</sup>C NMR (100 MHz, DMSO *d*<sub>6</sub>, δ ppm): 19.61, 24.50, (2CH<sub>3</sub>), 55.88 (OCH<sub>3</sub>), 61.57 (pyrazolone-CH<sub>2</sub>), 110.93, 114.52, 120.15, 122.39, 123.90, 129.88, 145.43, 146.21, 154.98, 157.39, 159.98, 161.58, 162.11 (Ar-C), 170.17 (C = O); MS, *m/z* (%): 418 (M<sup>+</sup>, 28); Anal. Calc. for C<sub>21</sub>H<sub>18</sub>N<sub>6</sub>O<sub>2</sub>S (418.48): Calcd. C, 60.27; H, 4.34; N, 20.08; S, 7.66; found C, 60.01; H, 4.06; N, 19.81; S, 7.38.

4.1.8.2. 5-Amino-2-(2-(furan-2-yl)-7,9-dimethylpyrido [3',2':4,5]thieno[3,2-d]pyrimidin-4-yl)-2,4-dihydro-3H-pyrazol-3-one (9b). Yield 78%, brownish powder, m.p. 225 °C, IR (KBr, *v*<sub>max</sub>/cm<sup>-1</sup>): 3208 (NH<sub>2</sub>), 3099 (CH-aromatic), 2933, 2843 (CH-aliphatic), 1677 (C = O); <sup>1</sup>H NMR (400 MHz, DMSO *d*<sub>6</sub>, δ ppm): 2.56 (s, 3H, CH<sub>3</sub>), 2.89 (s, 3H, CH<sub>3</sub>), 2.98 (s, 2H, pyrazolone-CH<sub>2</sub>), 6.64–8.02 (m, 4H, Ar-H), 9.73 (s, 2H, NH<sub>2</sub>, D<sub>2</sub>O exchangeable); <sup>13</sup>C NMR (100 MHz, DMSO *d*<sub>6</sub>, δ ppm): 19.87, 24.51 (2CH<sub>3</sub>), 65.59 (pyrazolone-CH<sub>2</sub>), 107.93, 110.91, 113.72, 122.19, 123.89, 145.45, 146.29, 151.99, 153.02, 154.67, 154.91, 159.98, 161.58 (Ar-C), 170.90 (C = O); MS, *m/z* (%): 378 (M<sup>+</sup>, 60); Anal. Calc. for C<sub>18</sub>H<sub>14</sub>N<sub>6</sub>O<sub>2</sub>S (378.41): Calcd. C, 57.13; H, 3.73; N, 22.21; S, 8.47; found C, 56.88; H, 3.48; N, 21.97; S, 8.18.

#### 4.1.9. Synthesis of 2-(pyridothienopyrimidin-4-yl)-5-methyl-2,4-dihydro-3H-pyrazol-3-one derivatives 10a,b

A mixture of compound **5a,b** (1 mmol), and ethyl acetoacetate (1 mmol) in ethanol/glacial acetic acid solution (1:1, 20 mL)

was refluxed for 10 h. Upon reaction completion, the mixture solution was concentrated, poured onto ice/water. The obtained solid was filtered, washed with water, and recrystallized from acetone to give the corresponding derivatives **10a,b**.

**4.1.9.1. 2-(2-(4-Methoxyphenyl)-7,9-dimethylpyrido[3',2':4,5]thieno[3,2-d]pyrimidin-4-yl)-5-methyl-2,4-dihydro-3H-pyrazol-3-one (10a).** Yield 90%, brownish powder, m.p. 241 °C; IR (KBr,  $\nu_{\max}/\text{cm}^{-1}$ ): 3089 (CH-aromatic), 2959, 2922, (CH-aliphatic), 1676 (C = O), 1590 (C = N);  $^1\text{H}$  NMR (400 MHz, DMSO  $d_6$ ,  $\delta$  ppm): 1.96 (s, 3H, CH<sub>3</sub>), 2.55 (s, 3H, CH<sub>3</sub>), 2.73 (s, 3H, CH<sub>3</sub>), 3.01 (s, 2H, pyrazolone-CH<sub>2</sub>), 3.83 (s, 3H, OCH<sub>3</sub>), 7.05 (d, 2H,  $J$  = 16.7 Hz, Ar-H), 7.21 (s, 1H, Ar-H), 8.36 (d, 2H,  $J$  = 16.4 Hz, Ar-H);  $^{13}\text{C}$  NMR (100 MHz, DMSO  $d_6$ ,  $\delta$  ppm): 18.93, 19.81, 24.95 (3CH<sub>3</sub>), 31.59 (pyrazolone-CH<sub>2</sub>), 55.85 (OCH<sub>3</sub>), 107.73, 114.12, 114.49, 122.40, 123.87, 129.73, 130.62, 145.47, 147.21, 160.01, 160.59, 161.62, 161.99 (Ar-C), 172.92 (C = O); MS,  $m/z$  (%): 417 (M<sup>+</sup>, 10); Anal. Calc. for C<sub>22</sub>H<sub>19</sub>N<sub>5</sub>O<sub>2</sub>S (417.49): Calcd. C, 63.29; H, 4.59; N, 16.78; S, 7.68; found C, 63.02; H, 4.34; N, 16.51; S, 7.39.

**4.1.9.2. 2-(2-(Furan-2-yl)-7,9-dimethylpyrido[3',2':4,5]thieno[3,2-d]pyrimidin-4-yl)-5-methyl-2,4-dihydro-3H-pyrazol-3-one (10b).** Yield 87%, brownish powder, m.p. 232 °C; IR (KBr,  $\nu_{\max}/\text{cm}^{-1}$ ): 3096 (CH-aromatic), 2962, 2921 (CH-aliphatic), 1674 (C = O), 1595 (C = N);  $^1\text{H}$  NMR (400 MHz, DMSO  $d_6$ ,  $\delta$  ppm): 2.26 (s, 3H, CH<sub>3</sub>), 2.62 (s, 3H, CH<sub>3</sub>), 2.72 (s, 3H, CH<sub>3</sub>), 2.97 (s, 2H, pyrazolone-CH<sub>2</sub>), 6.79–8.02 (m, 4H, Ar-H);  $^{13}\text{C}$  NMR (100 MHz, DMSO  $d_6$ ,  $\delta$  ppm): 18.72, 19.86, 24.91 (3CH<sub>3</sub>), 32.03 (pyrazolone-CH<sub>2</sub>), 107.72, 108.16, 112.14, 122.17, 123.81, 128.72, 130.15, 145.50, 147.21, 159.79, 161.50, 162.64, 163.93 (Ar-C), 172.57 (C = O); MS,  $m/z$  (%): 377 (M<sup>+</sup>, 74); Anal. Calc. for C<sub>19</sub>H<sub>15</sub>N<sub>5</sub>O<sub>2</sub>S (377.42): Calcd. C, 60.47; H, 4.01; N, 18.56; S, 8.49; found C, 60.30; H, 3.86; N, 18.38; S, 8.21.

#### 4.1.10. Synthesis of 4-(3,5-dimethyl-1H-pyrazol-1-yl)pyridothienopyrimidines **11a,b**

A mixture of compounds **5a,b** (1 mmol), and acetylacetone (1 mmol) in glacial acetic acid (10 mL) was refluxed for 8 h. After the reaction completion, the mixture solution was cooled, poured onto ice/water and the solid obtained was collected by filtration and recrystallized from acetone to give the corresponding derivatives **11a,b**.

**4.1.10.1. 4-(3,5-Dimethyl-1H-pyrazol-1-yl)-2-(4-methoxyphenyl)-7,9-dimethylpyrido[3',2':4,5]thieno[3,2-d]pyrimidine (11a).** Yield 86%, greenish powder, m.p. 248 °C; IR (KBr,  $\nu_{\max}/\text{cm}^{-1}$ ): 3087 (CH-aromatic), 2918, 2837 (CH-aliphatic), 1623 (C = N);  $^1\text{H}$  NMR (400 MHz, DMSO  $d_6$ ,  $\delta$  ppm): 2.31 (s, 3H, CH<sub>3</sub>), 2.59 (s, 3H, CH<sub>3</sub>), 2.85 (s, 3H, CH<sub>3</sub>), 2.99 (s, 3H, CH<sub>3</sub>), 3.85 (s, 3H, OCH<sub>3</sub>), 6.30 (s, 1H, pyrazole-H<sub>4</sub>), 7.05 (d, 2H,  $J$  = 8.4 Hz, Ar-H), 7.23 (s, 1H, Ar-H), 8.30 (d, 2H,  $J$  = 8.4 Hz, Ar-H);  $^{13}\text{C}$  NMR (100 MHz, DMSO  $d_6$ ,  $\delta$  ppm): 13.72, 16.21, 19.75, 24.70 (4CH<sub>3</sub>), 55.85 (OCH<sub>3</sub>), 108.33, 110.55, 114.63, 116.60, 122.55, 123.52, 131.10, 137.43, 140.45, 143.11, 145.47, 149.80, 155.76, 160.14, 161.62, 166.90 (Ar-C); MS,  $m/z$  (%): 415 (M<sup>+</sup>, 44); Anal. Calc. for C<sub>23</sub>H<sub>21</sub>-

N<sub>5</sub>OS (415.52): Calcd. C, 66.48; H, 5.09; N, 16.85; S, 7.72; found C, 66.21; H, 4.88; N, 16.58; S, 7.43.

**4.1.10.2. 4-(3,5-Dimethyl-1H-pyrazol-1-yl)-2-(furan-2-yl)-7,9-dimethylpyrido[3',2':4,5]thieno[3,2-d]pyrimidine (11b).** Yield 65%, brownish powder, m.p. 240 °C; IR (KBr,  $\nu_{\max}/\text{cm}^{-1}$ ): 3097 (CH-aromatic), 2966, 2919 (CH-aliphatic), 1620 (C = N);  $^1\text{H}$  NMR (400 MHz, DMSO  $d_6$ ,  $\delta$  ppm): 2.22 (s, 3H, CH<sub>3</sub>), 2.58 (s, 3H, CH<sub>3</sub>), 2.75 (s, 3H, CH<sub>3</sub>), 2.86 (s, 3H, CH<sub>3</sub>), 6.20 (s, 1H, pyrazole-H<sub>4</sub>), 6.67–7.89 (m, 4H, Ar-H);  $^{13}\text{C}$  NMR (100 MHz, DMSO  $d_6$ ,  $\delta$  ppm): 13.94, 15.96, 19.72, 24.71 (4CH<sub>3</sub>), 105.61, 110.50, 111.46, 112.83, 122.34, 123.88, 131.15, 137.40, 140.73, 142.58, 145.46, 152.19, 159.88, 160.97, 162.61, 166.60 (Ar-C); MS,  $m/z$  (%): 375 (M<sup>+</sup>, 100); Anal. Calc. for C<sub>20</sub>H<sub>17</sub>N<sub>5</sub>OS (375.45): Calcd. C, 63.98; H, 4.56; N, 18.65; S, 8.54; found C, 63.71; H, 4.31; N, 18.37; S, 8.82.

#### 4.2. Antimicrobial assay

All synthesized compounds were screened for their *in vitro* antimicrobial activity against five bacterial strains (*S. aureus* 25923, *B. subtilis* 6633, *B. cereus* 33018, *E. coli* 8739, *S. typhimurium* 14028), three yeasts (*C. albicans* 10231, *C. tropicalis* 750, *S. cerevisiae*) and two fungi (*Aspergillus flavus*, *Aspergillus niger* EM77). The diameter of inhibition zone (DIZ) assay was performed by agar disk diffusion method (Penna et al. 1998) and the (MIC) values were determined by using broth dilution method (Wiegand et al. 2008). More details were provided in the supplementary material.

#### 4.3. In vitro anticancer screening

The *in vitro* cytotoxicity potency of the target compounds **2a,b–11a,b** was screened against HepG-2 and MCF-7 cancer cell lines by MTT assay (van Meerloo et al., 2011). The cytotoxicity was estimated as IC<sub>50</sub> in  $\mu\text{M}$  for the tested compounds and the reference drugs (doxorubicin and cisplatin) listed in Table 3. More details were provided in Supplementary material.

#### 4.4. EGFR kinase inhibitory assay

EGFR<sup>WT</sup> kinase inhibitory assay was performed for the target compounds **2b**, **4a**, **6a**, **7b**, **7c**, and **9a** with erlotinib as a reference inhibitor, by using the EGFR<sup>WT</sup> kinase assay kit (Cat. # 40321), while compounds **6a**, **7b**, **7c** and **9a** were further tested against EGFR<sup>L858R</sup> and EGFR<sup>L858R</sup> using Kinase Assay Kit Catalog # 40,324 and EGFR(T790M) Kinase Assay Kit Catalog # 40,323 in comparison to erlotinib. The assay kit is designed to measure EGFR Kinase activity for screening applications using Kinase-Glo® MAX as a detection reagent using Kinase-Glo® MAX as a detection reagent. The luminescence was measured using the microplate reader (Infinite M200 microplate reader, Tecan, Männedorf, Switzerland) (Aiebchun et al., 2021). All assays were performed in triplicate and the relative inhibition (%) of inhibitors were then calculated compared to the control with no inhibitor. Then the IC<sub>50</sub> values (the concentration which provides 50% enzyme inhibition) and their standard deviation (SD) for the tested compounds and the reference drug were determined in ( $\mu\text{M}$ )

and listed in Table 4, 5. More details were provided in the supplementary material.

#### 4.5. Computational studies

##### 4.5.1. Molecular modeling studies

The molecular modeling studies were carried out using Molecular Operating Environment (MOE, 2019.0102) software. The RMSD gradient of  $0.1 \text{ kcal}\cdot\text{mol}^{-1}\text{\AA}^{-1}$  was reached using the MMFF94x force field and the partial charges were automatically calculated. (Yan et al. 2020; Stamos et al., 2002). More details were provided in the supplementary material.

##### 4.5.2. ADME study

SwissADME is a free web tool to evaluate pharmacokinetics, drug-likeness and medicinal chemistry friendliness of small molecules. <http://www.swissadme.ch/index.php>.

#### Declaration of Competing Interest

The authors declare that they have no known competing financial interests or personal relationships that could have appeared to influence the work reported in this paper.

#### Appendix A. Supplementary material

Supplementary data to this article can be found online at <https://doi.org/10.1016/j.arabjc.2022.103751>.

#### References

- Abdelaziz, M.E., El-Miligy, M.M.M., Fahmy, S.M., Mahran, M.A., Hazzaa, A.A., 2018. Design, synthesis and docking study of pyridine and thieno[2,3-*b*] pyridine derivatives anticancer PIM-1 kinase inhibitors. *Bioorg. Chem.* 80, 674–692. <https://doi.org/10.1016/j.bioorg.2018.07.024>.
- Aiebchun, T., Mahalapbutr, P., Auepattanapong, A., Khaikate, O., Seetaha, S., Tabtimmai, L., Kuhakarn, C., Choowongkamon, K., Rungrotmongkol, T., 2021. Identification of vinyl sulfone derivatives as egfr tyrosine kinase inhibitor: in vitro and in silico studies. *Molecules* 26 (8), 2211. <https://doi.org/10.3390/molecules26082211>.
- Al-Trawneh, S.A., Tarawneh, A.H., Gadetskaya, A.V., Seo, E., Al-Ta'ani, M.R., Al-Taweel, S.A., El-Abadelah, M.M., 2021. Synthesis and cytotoxicity of thieno[2,3-*b*]pyridine derivatives toward sensitive and multidrug-resistant leukemia cells. *Acta Chim. Solv.* 68(2), 458–465. [10.17344/acsi.2020.6609](https://doi.org/10.17344/acsi.2020.6609).
- Amorim, R., de Meneses, M.D.F., Borges, J.C., da Silva Pinheiro, L. C., Caldas, L.A., Cirne-Santos, C.C., de Mello, M.V.P., de Souza, A.M.T., Castro, H.C., de Palmer Paixão, I.C.N., Campos, R.M., Bergmann, I.E., Malirat, V., Bernardino, A.M.R., Rebello, M.A., Ferreira, D.F., 2017. Thieno[2,3-*b*]pyridine derivatives: a new class of antiviral drugs against Mayaro virus. *Arch. Virol.* 162 (6), 1577–1587. <https://doi.org/10.1007/s00705-017-3261-0>.
- Arabshahi, H.J., Rensburg, M.V., Pilkington, L.I., Jeon, C.Y., Song, M., Gridel, L.-M., et al, 2015. A synthesis, *in silico*, *in vitro* and *in vivo* study of thieno[2,3-*b*]pyridine anticancer analogues. *Med. Chem. Commun.* 6, 1987–1997. <https://doi.org/10.1039/C5MD00245A>.
- Aziz, Y.M.A., Said, M.M., El Shihawy, H.A., Abouzid, K.A., 2015a. Discovery of novel tricyclic pyrido [3', 2': 4, 5] thieno [3, 2-*d*] pyrimidin-4-amine derivatives as VEGFR-2 inhibitors. *Bioorg Chem.* 60, 1–12. <https://doi.org/10.1016/j.bioorg.2015.03.004>.
- Aziz, Y.M.A., Said, M.M., El Shihawy, H.A., Tolba, M.F., Abouzid, K.A.M., 2015b. Discovery of potent anti-proliferative agents targeting EGFR tyrosine kinase based on pyrido[3',2':4,5]thieno [3,2-*d*]pyrimidin-4-amine scaffold. *Chem. Pharm. Bull.* 63, 1015. <https://doi.org/10.1248/cpb.c15-00592>.
- El-Essawy, F.A., Boshta, N.M., El-Sawaf, A.K., Nassar, A.A., Khalafallah, M.S., 2016. Synthesis of novel 3-substituted pyridothienopyrimidine derivatives with biological evaluation as antimicrobial agents. *Chem. Res. Chin. Univ.* 32, 967–972. <https://doi.org/10.1007/s40242-016-6218-z>.
- Elmetwally, S.A., Saied, K.F., Eissa, I.H., Elkaced, E.B., 2019. Design, synthesis and anticancer evaluation of thieno[2,3-*d*]pyrimidine derivatives as dual EGFR/HER2 inhibitors and apoptosis inducers. *Bioorg. Chem.* 88. <https://doi.org/10.1016/j.bioorg.2019.102944>.
- El-Nassan, H.B., Naguib, B.H., Beshay, E.A., 2018. Synthesis of new pyridothienopyrimidinone and pyridothienotriazolopyrimidine derivatives as pim-1 inhibitors. *J. Enzyme Inhib. Med. Chem.* 33 (1), 58–66. <https://doi.org/10.1080/14756366.2017.1389921>.
- Eurtivong, C., Semenov, V., Semenova, M., Konyushkin, L., Atamanenko, O., Reynisson, J., Kiselyov, A., 2017. Identification of anticancer agents based on the thieno[2,3-*b*]pyridine and 1*H*-pyrazole molecular scaffolds. *Bioorg. Med. Chem.* 25 (2), 658–664. <https://doi.org/10.1016/j.bmc.2016.11.041>.
- Fayed, A.A., Amr, A.E.G.E., Al-Omar, M.A., Mostafa, E.E., 2014. Synthesis and antimicrobial activity of some new substituted pyrido [3', 2': 4, 5] thieno[3,2-*d*]pyrimidinone derivatives. *Russ. J. Bioorg. Chem.* 40, 308–313. <https://doi.org/10.1134/S1068162014030042>.
- Felicio, M.R., Silva, O.N., Gonçalves, S., Santos, N.C., Franco, O.L., 2017. Peptides with dual antimicrobial and anticancer activities. *Front. Chem.* 5, 5. <https://doi.org/10.3389/fchem.2017.00005>.
- Ge Zayda, M., Abdel-Rahman, A.A., El-Essawy, F.A., 2020. Synthesis and antibacterial activities of different five-membered heterocyclic rings incorporated with pyridothienopyrimidine. *ACS Omega* 5 (11), 6163–6168. <https://doi.org/10.1021/acsomega.0c00188>.
- Giménez, B.G., Santos, M.S., Ferrarini, M., Fernandes, J.P.S., 2010. Evaluation of blockbuster drugs under the rule-of-five. *Die Pharmazie-An Int. J. Pharm. Sci.* 65 (2), 148–152. <https://doi.org/10.1691/ph.2010.9733>.
- Ghattas, A.B.A.G., Khodairy, A., Moustafa, H.M., Hussein, B.R.M., 2015. Synthesis and biological evaluation of some novel thienopyridines. *J. Pharm. Appl. Chem.* 1(1), 21–26. <http://dx.doi.org/10.12785/jpac/010103>.
- Jänne, P.A., Yang, J.C.H., Kim, D.W., Planchard, D., Ohe, Y., Ramalingam, S.S., et al, 2015. AZD9291 in EGFR inhibitor-resistant non-small-cell lung cancer. *N. Engl. J. Med.* 372 (18), 1689–1699. <https://doi.org/10.1056/NEJMoa1411817>.
- Lainetti, P.d.F., Leis-Filho, A.F., Laufer-Amorim, R., Battazza, A., Fonseca-Alves, C.E., 2020. Mechanisms of resistance to chemotherapy in breast cancer and possible targets in drug.
- Liang, X., Yang, Q., Wu, P., He, C., Yin, L., Xu, F., Yin, Z., Yue, G., Zou, Y., Li, L., Song, X., 2021. The synthesis review of the approved Tyrosine kinase inhibitors for anticancer therapy in 2015–2020. *Bioorg. Chem.* 105011. <https://doi.org/10.1016/j.bioorg.2021.105011>.
- Liu, H., Li, Y., Wang, X.Y., Wang, B., He, H.Y., Liu, J.Y., Xiang, M. L., He, J., Wu, X.H., Yang, L., 2013. Synthesis, preliminary structure-activity relationships, and in vitro biological evaluation of 6-aryl-3-amino-thieno[2,3-*b*]pyridine derivatives as potential anti-inflammatory agents. *Bioorg. Med. Chem. Lett.* 23 (8), 2349–2352. <https://doi.org/10.1016/j.bmcl.2013.02.059>.
- Loidreau, Y., Marchand, P., Dubouilh-Benard, C., Nourrisson, M.R., Duflos, M., Lozach, O., Loaëc, N., Meijer, L., Besson, T., 2012. Synthesis and biological evaluation of N-arylbenzo [b] thieno [3, 2-*d*] pyrimidin-4-amines and their pyrido and pyrazino analogues as Ser/Thr kinase inhibitors. *Eur. J. Med. Chem.* 58, 171–183. <https://doi.org/10.1016/j.ejmech.2012.10.006>.
- Luo, X.Y., Wu, K.M., He, X.X., 2021. Advances in drug development for hepatocellular carcinoma: clinical trials and potential therapeutic targets. *J. Exp. Clin. Cancer Res.* 40, 172. <https://doi.org/10.1186/s13046-021-01968-w>.

- Lyseng-Williamson, K.A., 2010. Erlotinib: a pharmaco-economic review of its use in advanced non-small cell lung cancer. *Pharmacoeconomics*. 28 (1), 75–92. <https://doi.org/10.2165/10482880-000000000-00000>.
- Madhusudana, K., Shireesha, B., Naidu, V.G., Ramakrishna, S., Narsaiah, B., Rao, A.R., Diwan, P.V., 2012. Anti-inflammatory potential of thienopyridines as possible alternative to NSAIDs. *Eur. J. Pharm.* 678, 48–54. [10.1016/j.ejphar.2011.12.019](https://doi.org/10.1016/j.ejphar.2011.12.019).
- Mansour, H., 2020. Thiophenethieno[2,3-*b*]pyridine-chitosan nanorods; synthesis, characterization, BSA-Binding and kinetic interactions with BSA, antibacterial and in-vitro release studies. *J. Mol. Struct.* 1219. <https://doi.org/10.1016/j.carres.2020.107990> 128611.
- Masuda, H., Zhang, D., Bartholomeusz, C., Doihara, H., Hortobagyi, G.N., Ueno, N.T., 2012. Role of epidermal growth factor receptor in breast cancer. *Breast Cancer Res Treat.* 136 (2), 331–345. <https://doi.org/10.1007/s10549-012-2289-9>.
- Milik, S.N., Abdel-Aziz, A.K., Lasheen, D.S., Serya, R.A.T., Minucci, S., Abouzid, K.A.M., 2018. Surmounting the resistance against EGFR inhibitors through the development of thieno[2,3-*d*]pyrimidine-based dual EGFR/HER2 inhibitors. *Eur. J. Med. Chem.* 155, 316–336. <https://doi.org/10.1016/j.ejmech.2018.06.011>.
- Mohi El-Deen, E.M., Abd El-Meguid, E.A., Hasabelnaby, S., Karam, E.A., Nossier, E.S., 2019. Synthesis, docking studies, and in vitro evaluation of some novel thienopyridines and fused thienopyridine–quinolines as antibacterial agents and DNA gyrase inhibitors. *Molecules* 24 (20), 3650. <https://doi.org/10.3390/molecules24203650>.
- Mohi El-Deen, E.M., Abd El-Meguid, E.A., Karam, E.A., Nossier, E.S., Ahmed, M.F., 2020. Synthesis and biological evaluation of new pyridothienopyrimidine derivatives as antibacterial agents and escherichia coli topoisomerase II inhibitors. *Antibiotics* 9 (10), 695. <https://doi.org/10.3390/antibiotics9100695>.
- Morgillo, F., Corte, C.M.D., Fasano, M., Fortunato Ciardiello, F., 2016. Mechanisms of resistance to EGFR-targeted drugs: lung cancer. *ESMO Open* 11 1, (3). <https://doi.org/10.1136/esmoopen-2016-000060> e000060.
- Nasser, A.A., Eissa, I.H., Oun, M.R., El-Zahabi, M.A., Taghour, M.S., Belal, A., Saleh, A.M., Mehany, A.B., Luesch, H., Mostafa, A.E., Afifi, W.M., 2020. Discovery of new pyrimidine-5-carbonitrile derivatives as anticancer agents targeting EGFR WT and EGFR T790M. *Org. Biomol. Chem.* 18 (38), 7608–7634. <https://doi.org/10.1039/d0ob01557a>.
- Penna, C.A., Marino, S.G., Gutkind, G.O., Clavin, M., Ferraro, G., Martino, V., 1998. Antimicrobial activity of *Eupatorium* species growing in Argentina. *J. Herbs. Spices Med. Plants.* 5, 21–28.
- Phan, T.T., Tran, B.T., Nguyen, S.T., Ho, T.T., Nguyen, H.T., Le, V.T., Le, A.T., 2019. EGFR plasma mutation in prediction models for resistance with EGFR TKI and survival of non-small cell lung cancer. *Clin. Transl. Med.* 8 (1), 4. <https://doi.org/10.1186/s40169-019-0219-8>.
- Presti, D., Quaquerini, E., 2019. The PI3K/AKT/mTOR and CDK4/6 Pathways in Endocrine Resistant HR + /HER2- Metastatic Breast Cancer: Biological Mechanisms and New Treatments. *Cancers (Basel)* 11 (9), 1242. <https://doi.org/10.3390/cancers11091242>.
- Rizka, O.H., Teleb, M., Abu-Seriec, M.M., Shaabana, O.G., 2019. Dual VEGFR-2/PIM-1 kinase inhibition towards surmounting the resistance to antiangiogenic agents via hybrid pyridine and thienopyridine-based scaffolds: Design, synthesis and biological evaluation. *Bioorg. Chem.* 92. <https://doi.org/10.1016/j.bioorg.2019.103189> 103189.
- Sanad, S.M.H., Mekky, A.E.M., 2021. New pyrido[3',2':4,5]thieno [3,2-*d*]pyrimidin-4(3H)-one hybrids linked to arene units: synthesis of potential MRSA, VRE, and COX-2 inhibitors. *Can. J. Chem.* 99 (11), 900–909. <https://doi.org/10.1139/cjc-2021-0121>.
- Schnute, M.E., Anderson, D.J., Brideau, R.J., Ciske, F.L., Collier, S.A., 2007. 2-Aryl-2-hydroxyethylamine substituted 4-oxo-4, 7-dihydrothieno[2, 3-*b*]pyridines as broad-spectrum inhibitors of human herpesvirus polymerases. *Bioorg. Med. Chem. Lett.* 17, 3349–3353. <https://doi.org/10.1016/j.bmcl.2007.03.1>.
- Sharma, P., Kaur, S., Chadha, B.S., Kaur, R., Kaur, M., Kaur, S., 2021. Anticancer and antimicrobial potential of enterocin 12a from *Enterococcus faecium*. *BMC Microbiol.* 21 (1), 1–14. <https://doi.org/10.1186/s12866-021-02086-502>.
- Sharom, F.J., 1997. The P-glycoprotein efflux pump: how does it transport drugs? *J. Membrane Biol.* 160 (3), 161–175.
- Shah, R.R., Shah, D.R., 2019. Safety and tolerability of epidermal growth factor receptor (EGFR) tyrosine kinase inhibitors in oncology. *Drug Saf.* 42 (2), 181–198. <https://doi.org/10.1007/s40264-018-0772-x>.
- Shetty, S.R., Yeeravalli, R., Bera, T., Das, A., 2021. Recent advances on epidermal growth factor receptor as a molecular target for breast cancer therapeutics. *Anticancer Agents Med. Chem.* 21 (14), 1783–1792. <https://doi.org/10.2174/1871520621666201222143213>.
- Sirakanyan, S.N., Spinelli, D., Geronikaki, A., Hakobyan, E.K., Sahakyan, H., Arabyan, E., Zakaryan, H., Nersesyan, L.E., Aharonyan, A.S., Danielyan, I.S., Muradyan, R.E., Hovakimyan, A.A., 2019. Synthesis, antitumor activity, and docking analysis of new pyrido[3',2':4,5]furo(thieno)[3,2-*d*]pyrimidin-8-amines. *Molecules* 24, 3952. <https://doi.org/10.3390/molecules24213952>.
- Song, P., Yang, J., Li, X., Huang, H., Guo, X., Zhou, G., Xu, X., Cai, Y., Zhu, M., Wang, P., Zhao, S., Zhang, D., 2017. Hepatocellular carcinoma treated with anti-epidermal growth factor receptor antibody nimotuzumab: A case report. *Medicine (Baltimore)*. 96, (39). <https://doi.org/10.1097/MD.00000000000008122> e8122.
- Stamos, J., Sliwkowski, M.X., Eigenbrot, C., 2002. Structure of the epidermal growth factor receptor kinase domain alone and in complex with a 4-anilinoquinazoline inhibitor. *J. Biol. Chem.* 277 (48), 46265–46272. <https://doi.org/10.1074/jbc.M207135200>.
- Sung, H., Ferlay, J., Siegel, R.L., Laversanne, M., Soerjomataram, I., Jemal, A., Bray, F., 2021. Global cancer statistics 2020: GLOBOCAN estimates of incidence and mortality worldwide for 36 cancers in 185 countries. *CA Cancer J. Clin.* 71 (3), 209–249. <https://doi.org/10.3322/caac.21660>.
- Thomas, R., Weihua, Z., 2019. Rethink of EGFR in cancer with Its Kinase Independent function on board. *Front Oncol* 9, 800. <https://doi.org/10.3389/fonc.2019.00800>.
- van Meerloo, J., Kaspers, G.J., Cloos, J., 2011. Cell sensitivity assays: the MTT assay. *Methods Mol Biol.* 731, 237–245. [https://doi.org/10.1007/978-1-61779-080-5\\_20](https://doi.org/10.1007/978-1-61779-080-5_20).
- Wang, S., Cang, S., Liu, D., 2016. Third-generation inhibitors targeting EGFR T790M mutation in advanced non-small cell lung cancer. *J. Hematol. Oncol.* 9 (1), 1–7. <https://doi.org/10.1186/s13045-016-0268-z>.
- Wiegand, I., Hilpert, K., Hancock, R.E., 2008. Agar and broth dilution methods to determine the minimal inhibitory concentration (MIC) of antimicrobial substances. *Nat Protoc.* 3, 163–175. <https://doi.org/10.1038/nprot.2007.521>.
- Wu, C.H., Coumar, M.S., Chu, C.Y., Lin, W.H., Chen, Y.R., Chen, C.T., et al., 2010. Design and synthesis of tetrahydropyridothieno [2,3-*d*]pyrimidine scaffold based epidermal growth factor receptor (EGFR) kinase inhibitors: the role of side chain chirality and Michael acceptor group for maximal potency. *J. Med. Chem.* 53, 7316–7326. <https://doi.org/10.1021/jm100607r>.
- Wu, S., Zhu, W., Thompson, P., Hannun, Y.A., 2018. Evaluating intrinsic and non-intrinsic cancer risk factors. *Nat. Commun.* 9, 3490. <https://doi.org/10.1038/s41467-018-05467-z>.
- Yan, X.E., Ayaz, P., Zhu, S.J., Zhao, P., Liang, L., Zhang, C.H., Wu, Y.C., Li, J.L., Choi, H.G., Huang, X., Shan, Y., 2020. Structural basis of AZD9291 selectivity for EGFR T790M. *J. Med. Chem.* 63 (15), 8502–8511. <https://doi.org/10.1021/acs.jmedchem.0c00891>.
- Youssefyeh, R.D., Brown, R.E., Wilson, J., Shah, U., Jones, H., Loev, B., Khandwala, A., Leibowitz, M.J., Sonnino-Goldman, P., 1984. Pyrido [3', 2': 4, 5] thieno [3, 2-*d*]-N-triazines: A new series of orally active antiallergic agents. *J. Med. Chem.* 27 (12), 1639–1643. <https://doi.org/10.1021/jm00378a019>.